AAPM REPORT NO. 125

Functionality and Operation of Fluoroscopic Automatic Brightness Control/Automatic Dose Rate Control Logic in Modern Cardiovascular and Interventional Angiography Systems

A Report of AAPM Task Group 125 Radiography/Fluoroscopy Subcommittee, Imaging Physics Committee, Science Council

June 2012

ISBN: 978-1-936366-16-3
ISSN: 0271-7344

Published by

American Association of Physicists in Medicine
One Physics Ellipse
College Park, MD 20740-3846

Task Group 125

Co-Chairmen

Pei-Jan Paul Lin
Beth Israel Deaconess Medical Center, Boston MA 02115

Phillip Rauch
Henry Ford Health System, Detroit, MI 48202

Task Group Members

Stephen Balter
Columbia University Medical Center, New York, NY 10032

Atsushi Fukuda
Shiga Medical Center for Children, Moriyama City, Shiga-Ken, Japan 524-0022

Allen Goode
University of Virginia Health Science Center, Charlottesville, VA 22908

Gary Hartwell
University of Virginia Health Science Center, Charlottesville, VA 22908

Terry LaFrance
Baystate Health Systems, Inc., Springfield, MA 01199

Edward Nickoloff
Columbia University Medical Center, New York, NY 10032

Jeff Shepard
University of Texas M.D. Anderson Cancer Center, Houston, TX 77030

Keith Strauss
Cincinnati Children's Hospital Medical Center, Cincinnati, OH 45229

This page intentionally left blank.

Contents

Abstract

Task Group 125 (TG-125) was charged with investigating the functionality of fluoroscopic Automatic Dose Rate and Image Quality control logic in modern angiographic systems, paying specific attention to the spectral shaping filters and variations in the selected radiologic imaging parameters. The task group was also charged with describing the operational aspects of the imaging equipment for the purpose of assisting the clinical medical physicist with clinical setup and performance evaluation. Although there are clear distinctions between the fluoroscopic operation of an angiographic system and its acquisition modes (digital cine, digital angiography, digital subtraction angiography, etc.), the scope of this work was limited to the fluoroscopic operation of the systems studied.

The use of spectral shaping filters in cardiovascular and interventional angiography equipment has been shown to reduce patient dose. If the imaging control algorithm were programmed to work in conjunction with the selected spectral filter, and if the generator parameters were optimized for the selected filter, then image quality could also be improved. Although assessment of image quality was not included as part of this report, it was recognized that for fluoroscopic imaging the parameters that influence radiation output, differential absorption, and patient dose are also the same parameters that influence image quality. Therefore this report will utilize the terminology "Automatic Dose Rate and Image Quality" (ADRIQ) when describing the control logic in modern interventional angiographic systems and, where relevant, will describe the influence of controlled parameters on the subsequent image quality.

A total of 22 angiography units were investigated by the task group and, of these, one each was chosen as representative of the equipment manufactured by GE Healthcare, Philips Medical Systems, Shimadzu Medical USA, and Siemens Medical Systems. All equipment, for which measurement data were included in this report, was manufactured within the 3-year period from 2006 to 2008.

Using polymethylmethacrylate (PMMA) plastic to simulate patient attenuation, each angiographic imaging system was evaluated by recording the parameters Tube Potential in units of kilovolts peak (kVp), Tube Current in units of milliamperes (mA), Pulse Width (PW) in units of milliseconds (ms), spectral filtration setting, and Patient Air Kerma Rate (PAKR) as a function of the attenuator thickness. Data were graphically plotted to reveal the manner in which the ADRIQ control logic responded to changes in object attenuation. There were similarities in the manner in which the ADRIQ control logic operated that allowed the four chosen devices to be divided into two groups, with two of the systems in each group. There were also unique approaches to the ADRIQ control logic that were associated with some of the systems, and these are described in the report. The evaluation revealed relevant information about the testing procedure and also about the manner in which different manufacturers approach the utilization of

spectral filtration, pulsed fluoroscopy, and maximum PAKR limitation. This information should be particularly valuable to the clinical medical physicist charged with acceptance testing and performance evaluation of modern angiographic systems.

Key words: operational logic, fluoroscopy, filtration, Automatic Dose Rate Control, Automatic Brightness Control, patient exposure, acceptance testing, angiography.

I. Introduction

The use of spectral shaping filters in the fluoroscopic imaging procedures of cardiovascular and interventional angiography equipment has been shown to reduce Patient Air Kerma (PAK) while maintaining fluoroscopic image quality and extending the dynamic range in patient thickness.[1–5] Traditional x-ray image intensifier (XRII) fluoroscopic imaging systems have served an important role in medical imaging for many decades. With these imaging systems the operator controlled the exposure production via a footswitch while observing the dynamic image display through an optical lens or television display. Whenever the footswitch was activated, the x-ray production was continuous. These systems had many limitations that rigidly linked the image quality and the associated patient dose (Figure 1). The factors that played a role in limiting XRII imaging performance included a single, pre-set image intensifier input exposure rate; a fixed optical aperture; limited image processing; predefined image display parameters, fixed beam filtration, the use of anti-isowatt power curves, and limitations in the rate of heat input to the x-ray tube. Examples of traditional generator control curves are shown in Figure 2. With the optical aperture and filtration fixed, and with the x-ray production in continuous mode, the only generator parameters being controlled were the kVp and the mA. The x-ray generator control curve could thus be simply described in a plot of the kVp versus the mA. As the patient size changed, or the image was magnified via switching to a smaller field of view (FOV), the output brightness would change and the x-ray generator would have to respond. The control curves were a means of defining exactly how the generator would respond to adjust the kVp and mA as needed to maintain the output signal. These curves were called "anti-isowatt" because the kVp and mA increased or decreased simultaneously. For a given curve, when the kVp and mA reached the

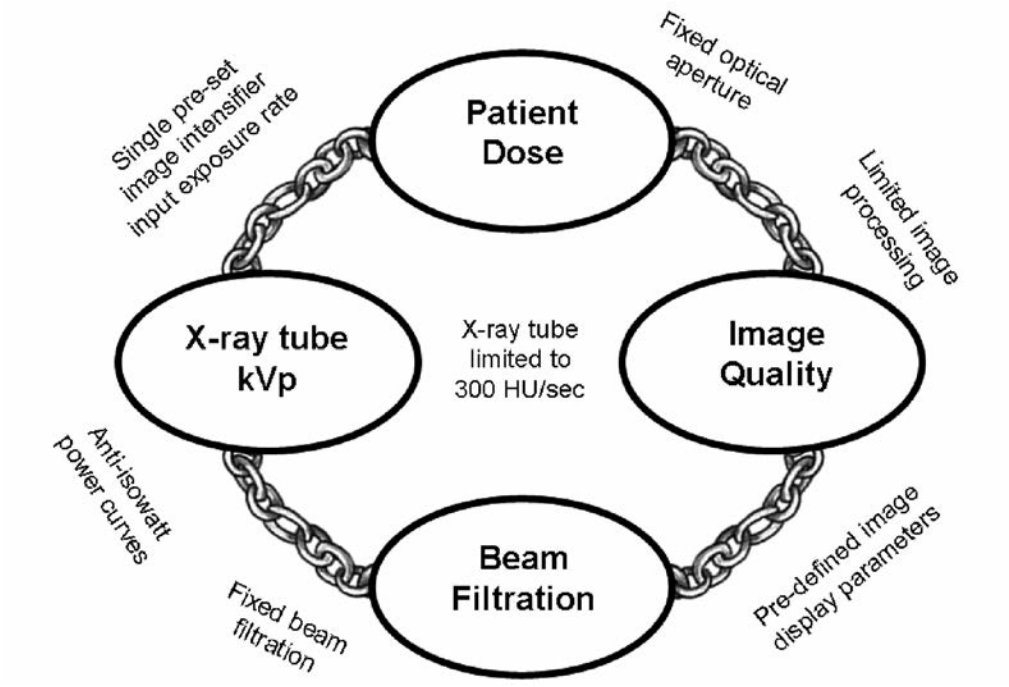

Figure 1. Limiting factors that keep patient dose and image quality rigidly linked in a manner that causes image quality to decrease as patient dose is reduced.

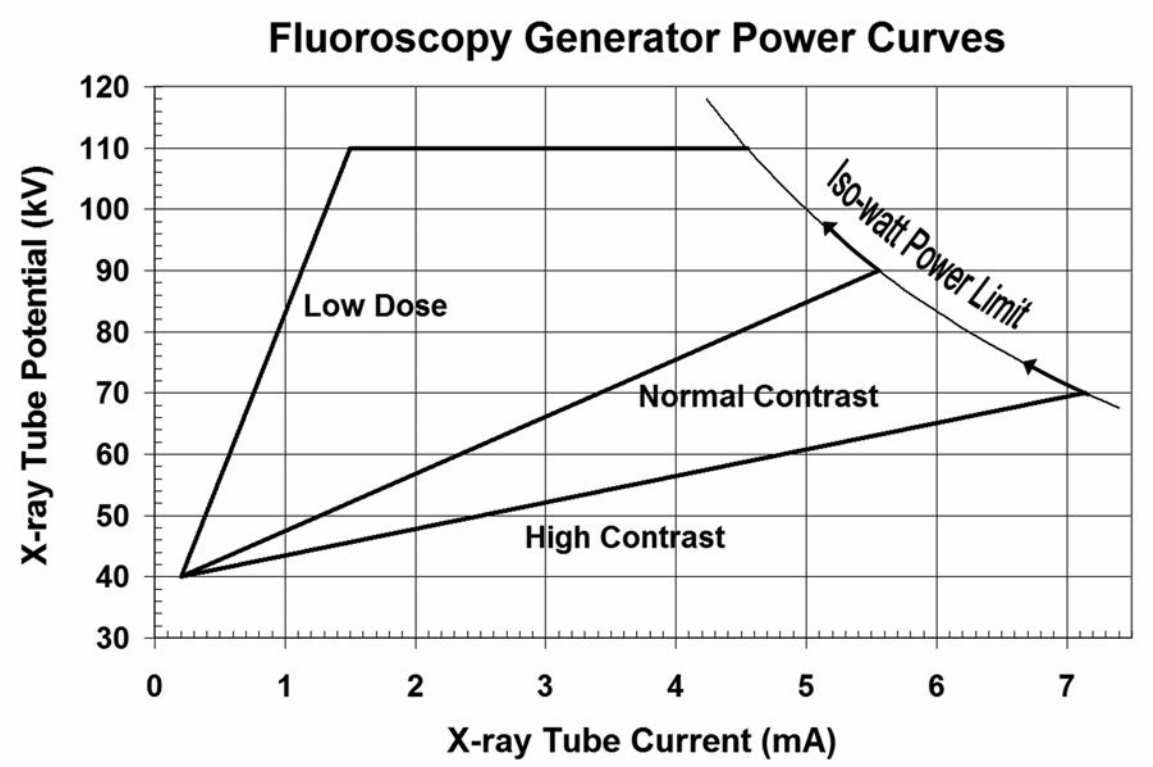

Figure 2. Traditional fluoroscopy x-ray generator control curves. The x-ray generator will follow the selected curve in response to a demand for more or less brightness at the output phosphor of the image intensifier.

limit of x-ray tube loading, the curve automatically switched to isowatt control. Along the isowatt line, the kVp increases while the mA decreases such that the product of kVp and mA remains constant.

For the sample curves of Figure 2, if the operator was interested in greater contrast in the image, the "High Contrast" control curve would be selected and the generator would favor a lower kVp. In comparison, selection of the "normal" contrast curve would result in a higher kVp for the same patient and procedure but would also result in a loss of image contrast. With this type of control, the most common means of reducing patient dose was to utilize a high kVp setting (Low Dose Curve in Figure 2), but this resulted in a lower differential absorption and an increased scatter fraction, both of which negatively impacted the image quality.

As shown in Figure 3, moving objects imaged with continuous fluoroscopy were blurred over the integration time of the image, which was 33.3 ms. Also note that the contrast was degraded. Modern fluoroscopy systems employ pulsed fluoroscopy, which has the potential to improve temporal resolution via the use of a short PW.[6] However, with pulsed fluoroscopy, caution must be taken to ensure that the PW does not exceed a value that would introduce image degradation effects.[7,8] Modern systems also have the means of controlling the XRII optical aperture, the PW, the beam filtration, and even the input dose to the detector, in addition to controlling the kVp and mA generator parameters. The control of additional parameters beyond kVp and mA make modern systems more complex. However, understanding how the modern Automatic Brightness Control/Automatic Dose Rate and Image Quality Control Logic (ABC/ADRIQ) logic functions is integral to any attempt to optimize the balance between patient dose and image quality.

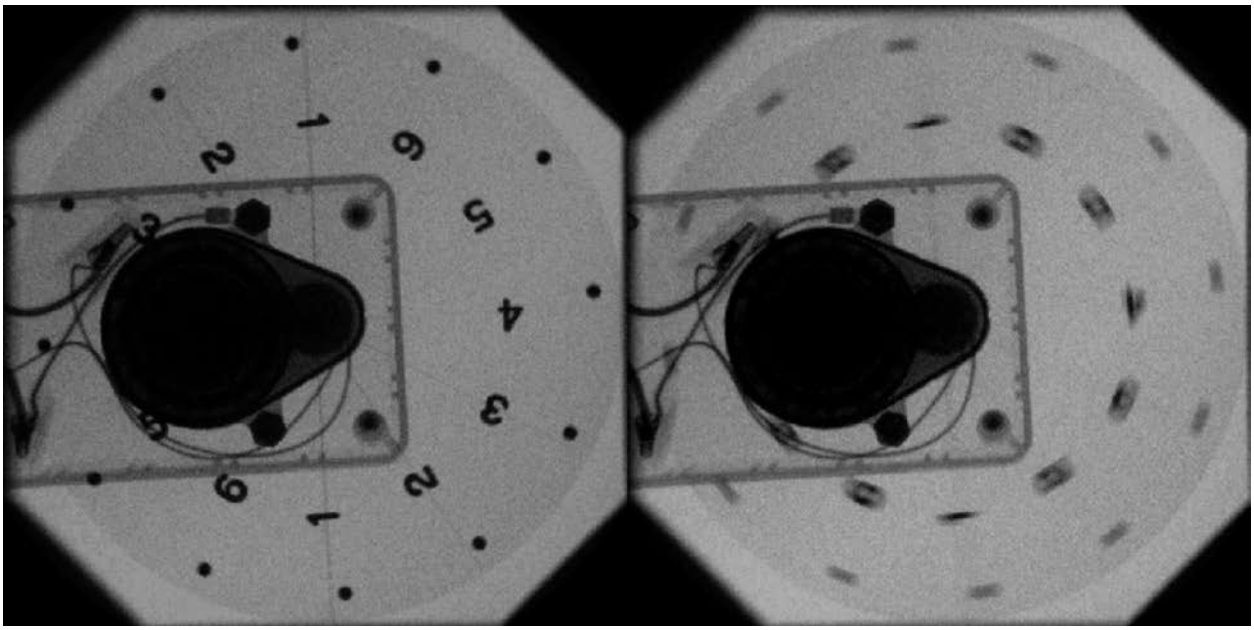

Figure 3. Pulsed versus continuous fluoroscopy. With pulsed fluoroscopy (left) the x-rays are produced for only a few milliseconds and temporal resolution was improved. With continuous fluoroscopy (right) each image frame was integrated over 33.3 ms and motion blur degrades the image. Also note the loss of contrast associated with the small black circles.

II. Task Group Charge

TG-125 was established and charged with two specific purposes. The first was to explore and investigate the functionality of fluoroscopic ABC/ADRIQ in modern cardiovascular and interventional angiography systems (hereafter designated "angiography systems"); that is, to investigate the operation of newer systems currently on the market and from a variety of manufacturers, paying specific attention to the spectral shaping filters and variations in the selected radiologic imaging parameters. The scope of this work was limited to the fluoroscopic operation of these systems.

The second purpose was to describe the operational aspects of the imaging equipment for the purpose of assisting the clinical medical physicist with clinical setup and performance evaluation. This report will provide an understanding of how generator control logic, aggressive spectral filtration, and imaging parameters are programmed to work together to maintain or to improve image quality while reducing the patient skin dose.

It is the opinion of the task group that a thorough understanding of ABC/ADRIQ is essential to the proper assessment of a modern fluoroscopic imaging system performance. For example, with modern fluoroscopy equipment the measurement of the radiation beam quality under clinically relevant conditions may yield an unexpectedly high value for the half-value layer (HVL). The clinical physicist must understand that this result is due to combinations of relatively thick spectral filtration and associated low kVp setting, and that this combination is an essential part of the means by which patient skin dose can be reduced while maintaining or even improving image quality. The clinical physicist must also be cognizant of the fact that the combinations of kVp and filter thickness are considerably different from those that are utilized by radiation

dosimeter calibration laboratories, and that the calibration of ionization chambers and solid-state detectors becomes an issue. At the time of this writing, there was no calibration beam available from any of the national calibration laboratories that matched the beam qualities of those employed by the angiography equipment included in this study. The lack of properly calibrated radiation detectors for the accurate measurement of air kerma makes estimation of PAK and PAKR more difficult.

III. Radiation Exposure

Since the parameters that are utilized by the ABC/ADRIQ control logic to maintain a constant average detector signal are also the same parameters that govern the x-ray tube output intensity and photon energy spectrum, we need to consider the types of radiation exposure involved in fluoroscopic imaging. There are four types of radiation exposure of interest when considering fluoroscopy as a visualization device for diagnostic and therapeutic procedures: (1) the Entrance Exposure Rate to the Detector (EERD), (2) the nominal patient Skin Entrance Exposure Rate (SEER), (3) the maximum patient SEER, and (4) the scattered radiation from the patient and other materials in the path of the x-ray beam.

III.A. Entrance Exposure Rate to the Detector

For both XRII and flat-panel imaging detectors the photon energy distribution of the radiation incident on the detector, the spectral sensitivity of the detector, the energy conversion efficiency, and the spatial sampling array will determine the absorbed energy fluence per picture element (pixel) at the input to the detector's radiation capture layer. These factors together will determine the intensity of the output signal per pixel. Statistical fluctuations in the pixel-to-pixel output signal will determine the image quantum mottle and, in conjunction with the Detective Quantum Efficiency (DQE), the Signal to Noise Ratio (SNR) in the resultant image. If the EERD is too low, the image will suffer from increased noise; if too high, the patient dose will be unnecessarily high, although the image quality (SNR^2) will be improved. There are no regulations governing the EERD and the measured values obtained from a survey conducted by American Association of Physicists in Medicine (AAPM) Task Group 11 revealed a very wide range of values, ranging from 0.18 microgray per second (μGy/s) [20 microroentgen per second (μR/s)] to 9.1 μGy/s (1043 μR/s) for fluoroscopy systems in clinical use.[9] To provide a logical and reasonable guide to the selection of an appropriate value for the EERD, Phillip Rauch has proposed a simple rule of thumb, which he calls the "30-30-30 Rule."[10] This rule, and its name, has its basis in legacy XRII/Television fluoroscopy systems that operated in the continuous mode.[†] Recalling that standard National Television System Committee (NTSC)[11] video operates at 30 video frames per second (fps), Rauch created the rule by applying the value of 30 to the diameter of the input to the XRII, in units of centimeters (cm), and to the XRII input exposure

[†]Since the 30-30-30 rule has its basis in the operation of legacy fluoroscopy equipment and since a critical component of the rule is the value of EERD equal to 30 μR/s, the conversion to SI units is not shown in this part of the discussion.

rate (in units of μR/s). That is, for XRII-based continuous fluoroscopy at 30 video fps, with a 30-cm diameter FOV, the starting point for setting the EERD should be a nominal 30 μR/s. This is not a hard and fast rule, and the actual EERD can be allowed to vary from the 30 μR/s nominal value, depending on the noise tolerance of the interventionalist and the nature of the examination. For conventional XRII-based fluoroscopy systems without additional spectral beam shaping, acceptable values for the starting point would be in the range from 20 μR/s [175 nanograys per second (nGy/s)] to 90 μR/s (788 nGy/s) [i.e., 0.67 to 3 times the 30 μR/s (263 nGy/s) guideline], with the higher values only applied when the imaging task demands less noise. During fluoroscopy, flat-panel detectors will demand from 2 to 4 times the EERD required of a conventional image intensifier due to size of the pixels and the electronic noise arising in the active matrix readout array.[12,13,14] Because of this limitation and associated increased dose, flat-panel detectors should not be utilized without incorporation of aggressive spectral filtration. During single-frame or serial acquisition imaging, which utilizes a much higher detector input dose per frame, the flat-panel detector can operate at a slightly lower EERD than that of an image intensifier.

III.B. Nominal Patient Skin Entrance Exposure Rate

Discussions of SEER would normally be accompanied by a discussion of the fluoroscopic image quality.[15,16] However, owing to the complexity of the imaging control logic (e.g., as many as 60 parameters are controlled in order to ensure optimization of image quality[17]), a suitable imaging phantom would need to be defined that would be capable of assessing image quality with any commercially available imager and without bias. The phantom would have to be clinically relevant, yet it must not adversely affect the operation of the control logic. Although the task group considered the possibility that the NEMA-SCAI phantom,[18] could be suitable for this purpose, it was clear that some effort would be needed to ensure that the phantom provides a fair and accurate assessment. Ultimately, it was decided by TG-125 to recommend that assessment of image quality be removed from the original charge and to focus only on the operation of the ABC/ADRIQ control logic. On the other hand, it must be recognized that for fluoroscopic imaging the control parameters that influence radiation output, differential absorption, and patient dose are also the same parameters that influence the subsequent image quality.[19] Therefore this report will continue to utilize the terminology ADRIQ when describing the control logic in modern interventional angiographic systems and, where relevant, will describe the influence of controlled parameters on image quality.

The patient SEER depends on the generator operating curve, especially the way the kVp changes with increased attenuation. It also depends on the spectral filtration, the source-to-skin distance, the patient table attenuation, the table pad attenuation,[20] the grid bucky factor, the patient size, and the path length of the x-ray beam through the patient. Motz and Danos,[21] and later Zamenhof,[22] were able to demonstrate that the image information content per SEER, i.e., the ratio of the SNR^2 divided by the SEER, could be optimized by finding an appropriate combination of filtration and kVp. Onnasch et al.[23] further demonstrated that the contrast-to-noise ratio was independent of the filter thickness. Thus, thicker spectral filters could be utilized to reduce SEER, while lower kVp could be utilized to improve image contrast. This approach, along with the appropriate selection of detector input exposure per image frame, will result in

the desired improvement in image quality while at the same time reducing the patient skin dose. This concept was the principle behind the design and operation of modern ABC/ADRIQ control logic.

Contrary to popular belief, the SEER does *not* depend on the EERD, as demonstrated in Figure 4. In this figure the experimentally derived values of kVp and mA that would deliver an EERD of 788 nGy/s with 20 cm water as the attenuator are shown. Likewise, the values of kVp and mA that produce a SEER of 22 milligrays per minute (mGy/min) and those that produce a SEER of 44 mGy/min were also plotted. The circles identify the points where the SEER plots cross the EERD plot. At these two points the dose delivered to the detector were identical, but the SEER value differed by a factor of 2×.

This figure could also be used to illustrate one of the main principles that govern the utilization of beam spectral shaping in modern ABC/ADRIQ systems. In a simple field experiment we could acquire and plot a similar set of data by manually manipulating the x-ray generator parameters while adding filtration and monitoring the EERD and the SEER. Direct your attention to the lower circled crossing point in Figure 4. The SEER was a higher value than that corresponding to the other circled crossing points due mainly to the lower kVp. On the other hand, the lower kV would result in an increased image contrast at this operating point. If we now add

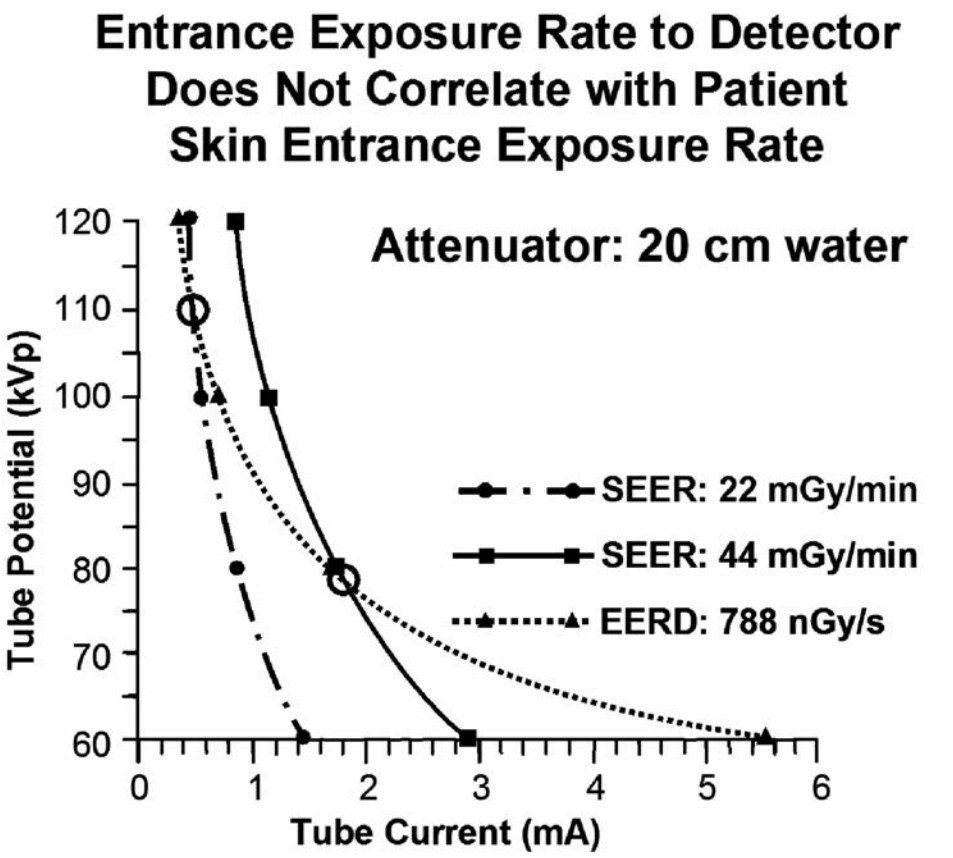

Figure 4. Experimental determination of the kVp and mA required to keep the EERD at 788 nGy/s with 20 cm water attenuator, and also the requirements to keep the SEER at 22 mGy/min and at 44 mGy/min. The circles indicate the values of kVp and mA that will provide exactly the same EERD but with patient doses differing by a factor of 2×. (Adapted from reference 49.)

filtration to the x-ray beam, without allowing the kVp and mA to change, then clearly the EERD will drop below the desired setting due to both spectral and intensity changes to the radiation reaching the detector. If we next keep the kVp constant but adjust the mA to deliver the same absorbed energy fluence per pixel at the detector input, the net result will be the same average detector output signal, but with a lower SEER due to the spectral absorption effects of the filter. If the measured new value of SEER was not as low as desired, we can add an additional increment of filtration and repeat the above procedure until we reach either the desired SEER or the generator power limit. In the latter case, where the combination of water thickness, filtration, kVp, and generator power limit does not permit achievement of the EERD, then we would need to use a higher kVp for that combination of settings. By doing this procedure using a number of different water thicknesses, we can create a generator control curve that will, for any given water equivalence, maintain the detector absorbed energy fluence per pixel using the values of spectral filtration and kVp determined during the experiment, and without exceeding the x-ray tube power limit. The net result should be the same or reduced SEER while maintaining acceptable image noise, *and* with equal or better image quality due to the lower kVp. This report will illustrate the manner in which various manufacturers have created combinations of spectral filtration and generator control curves to optimize their imaging systems. For the clinical medical physicist, having the knowledge and understanding of all of the parameters that impact patient dose is important since these factors are multiplicative, not additive.[24]

III.C. Maximum Patient Skin Entrance Exposure Rate

III.C.1. Regulatory Limits

The U.S. Food and Drug Administration (FDA), in Title 21CFR(1020.32),[25] has established regulatory limits on the maximum Air Kerma Rate (AKR) produced by fluoroscopy imaging equipment. The nominal limits are 88 mGy/min (10 R/min) for normal ABC/ADRIQ operation and 176 mGy/min (20 R/min) if an optional "high-level" control mode is provided. The limits must be measured under scatter-free conditions and are determined at a specifically defined measurement point which depends on the type of equipment. It should be noted that exceptions to these limits are allowed, based on the equipment manufacture date, on whether images are recorded, and on the source–to–image receptor distance (SID). The reader should consult the regulations to determine the limits associated with a specific piece of equipment.

III.C.2. Measurement Point[†]

(i) If the source is below the x-ray table, the AKR shall be measured at 1 cm above the tabletop or cradle.

(ii) If the source is above the x-ray table, the AKR shall be measured at 30 cm above the tabletop with the end of the beam-limiting device or spacer positioned as closely as possible to the point of measurement.

[†]Adapted from reference 25.

(iii) In a C-arm type of fluoroscope, the AKR shall be measured at 30 cm from the input surface of the fluoroscopic imaging assembly, with the source positioned at any available SID, provided that the end of the beam-limiting device or spacer is no closer than 30 cm from the input surface of the fluoroscopic imaging assembly.

(iv) In a C-arm type of fluoroscope having an SID less than 45 cm, the AKR shall be measured at the minimum SSD.

(v) In a lateral type of fluoroscope, the AKR shall be measured at a point 15 cm from the centerline of the x-ray table and in the direction of the x-ray source with the end of the beam-limiting device or spacer positioned as closely as possible to the point of measurement. If the tabletop is movable, it shall be positioned as closely as possible to the lateral x-ray source, with the end of the beam-limiting device or spacer no closer than 15 cm to the centerline of the x-ray table.

III.C.3. SID Output Compensation

A lesser-known feature of fluoroscopy systems, the SID output compensation, will be briefly described. As the SID is varied, this control circuit adjusts the maximum radiation output, determined at the FDA-specified measurement point, in accordance with the x-ray tube load limits and the regulatory maximum exposure rate requirements. In particular, the SID compensation circuit is designed to automatically adjust the maximum kVp and mA values such that the maximum radiation dose rate at the specified measurement point is maintained at the regulatory limit, irrespective of the SID. Since the tabletop height (and thus the patient skin entrance point) is not necessarily raised or lowered in conjunction with changes in the position of the image receptor, the maximum fluoroscopic output at the location of the patient's skin may "appear" to exceed the regulatory limits. In fact, since the maximum output is measured at the location defined by the FDA, the compensation adjustments will ensure that the limits *at that location* are not exceeded. On the other hand, if a large SID is utilized while the patient's skin entry point is close to the x-ray source, the *actual* maximum SEER can be an order of magnitude higher than that specified by the FDA. If the SID output compensation is not properly calibrated there may be some SID settings where the maximum exposure rate will exceed the 88 mGy/min or 176 mGy/min values. It is therefore important for the clinical medical physicist to be aware of this potential for increased skin dose and to educate both administrators[26] and users[27] regarding the potential for skin injury and the means to avoid this hazard.

III.C.4. Critical Lead Thickness and Automatic Shutoff of Fluoroscopy

When determining the maximum dose rate at the FDA-specified measurement point, it is important to consider that for some fluoroscopy systems the use of a lead sheet as a beam stop may inhibit the achievement of the desired maximum generator settings. This will occur when the manufacturer has incorporated a threshold value of detector signal that must be achieved. If the minimum signal is not reached, the system will cease the fluoroscopic exposure and indicate an error via a message on the image display monitor or on the operator's control screen. For such systems when the lead beam stop is too thick the generator, under ABC/ADRIQ control, will not

reach the combination of kVp, mA, and PW that produces the maximum output. For such systems there will be a critical lead thickness (CLT) below which the minimum threshold detector signal is reached, but above which the signal is insufficient. When the beam stop is set to the CLT, the brightness of the displayed fluoroscopy image might still be maintained by the television Automatic Gain Control (AGC). Beyond the point where the video signal gain has reached the maximum value, the system will achieve only a fraction of the desired display brightness.

When the beam stop is thinner than the CLT, the system logic will operate normally, but the generator's settings will be less than the maximum allowed. Attenuators such as aluminum (Al), copper (Cu), or lead (Pb) sheets traditionally employed by medical physicists to determine the maximum output of fluoroscopy systems might be either too thin to reach the CLT or too thick so that the fluoroscopy system is turned off, preventing the measurement of the maximum radiation output.

Measurement of the maximum output must therefore be carried out with care, and the appropriate thickness of attenuator is essential. The CLT equivalent for materials other than lead could correspond to a total of 15 to 16 inches of PMMA plastic plates, or more than 14 mm of Cu. The use of PMMA or other thick attenuators, however, is not recommended for this measurement since the conditions for maximum entrance exposure rate require that no scattered radiation reach the radiation dosimeter. A suitable approach would be to have several thicknesses of lead sheet available ranging from 0.25 mm to 2 mm. Alternatively, the use of lead-aprons or lead-equivalent aprons can be effectively utilized to achieve the maximum output operating condition.

III.D. Scattered Radiation

As previously mentioned, the use of spectral beam shaping will serve to reduce the SEER. An added bonus is that although the scatter fraction increases due to beam hardening, the actual scatter intensity is reduced.[28] Thus, there is a dose reduction benefit to the personnel conducting the interventional procedure as well as that for the patient.

IV. Spectral Filtration

The value in using spectral filters made of Al (Z=13) or Cu (Z=29) as a means of reducing patient dose was recognized and documented in the early 1950s,[29,30] and today spectral shaping filters may be found on typical radiographic equipment as well as conventional fluoroscopy systems.[31–35] In addition to Al and Cu, many other elements have also been investigated such as

- Titanium (Z=22), Niobium (Z=41), Tin (Z=50), Samarium (Z=62), Erbium (Z=68), Tungsten (Z=74), Gold (Z=79), and Uranium (Z=92)[36]
- Samarium (Z=62), Gadolinium (Z=64), and Erbium (Z=68)[37]
- Tin (Z=50), Lanthanum (Z=57), Gadolinium (Z=64), Erbium (Z=68), and Lutecium (Z=71)[38]
- Erbium (Z=68) and Samarium (Z=62)[39]
- Hafnium (Z=72)[40]

- Tantalum (Z=73)[41,42]
- Niobium (Z=41)[43]
- Samarium (Z=62), Gadolinium (Z=64), Holmium (Z=67), Ytterbium (Z=70), and Tungsten (Z=74).[44]

Although the list of potential filter materials is large, Nickoloff[45] showed that for elements with atomic number less than 42, equivalent x-ray spectra can be obtained by substituting Cu of appropriate thickness. He also showed that Cu was more efficient than Al, where the efficiency was defined as the percentage of photons in the unfiltered x-ray beam that pass though the material when the amount of filtration was adjusted such that the average photon energy was the same.

The incorporation by manufacturers of spectral shaping filters into the equipment design began as interventional angiography procedures became widely practiced in the United States in the early 1990s.[46–48] All equipment investigated by the task group utilized combinations of Al and Cu filtration. Two manufacturers make use of at least one high atomic number filter material in addition to utilizing combinations of Cu and Al. Shimadzu used a combination of gold (Au) and Al, and Toshiba used tantalum (Ta).

It is clearly evident from the experimental studies of the various spectral filters cited above that the widespread use of spectral shaping filters has contributed to a reduction in patient skin dose. Furthermore, the application of specialized x-ray generator control curves, along with improvements in noise reduction techniques and image processing algorithms, have been instrumental in maintaining an acceptable level of image quality whenever spectral shaping filters are utilized.[49]

There are two general approaches to the implementation of spectral beam filtration in fluoroscopy. For lack of established terminology, the first approach shall be called the "Traditional Method"; the second shall be called the "Program-Switched Method." The program-switched method can then be further divided into two distinct methods. In this report the first of these is referred to as the "Anatomical Program Based Filter Selection," and the second shall be called the "Seissl Method" after the Siemens engineer Johann Seissl, who patented the original scheme of using automatically varying thicknesses of Cu filtration[†] in 1997.[50]

IV.A. Traditional Method of Filter Selection

The traditional method utilizes combinations of filter materials which are fixed in the collimator, cannot be varied by the user, and do not change with the anatomical program selected. The traditional method has been utilized in legacy fluoroscopic systems for many decades and is commonly employed today in mobile vascular C-arms utilized in the surgical suite, and in many fixed, non-vascular fluoroscopy systems.

[†]J. Seissl, personal communications on "Comprehensive application of copper filters for cardiovascular angiography systems" and Siemens Medical Systems internal memorandums (1999).

IV.B. Program-Switched Method of Filter Selection

IV.B.1. Anatomical Program–Based Filter Selection

The Program-Switched Method is an automated form of the traditional method in that predetermined combinations of added spectral filtration can be automatically switched under program control. With this method the type of filter material and/or the thickness is determined via user selection of an anatomically or procedurally based exposure program. The filter selected can also be dependent on the SID, or it can be linked to one of the fluoroscopy exposure rate control settings. Two or more fluoroscopy exposure rate control settings (fluoroscopy dose modes) are generally provided. These are often selectable by the user on the tableside control module. These selections correspond to predefined values of fluoroscopy pulse rate, EERD, x-ray generator control curve, and spectral filtration. Once a fluoroscopy mode is selected, the spectral filtration is set and is independent of the variations in patient attenuation. During fluoroscopic operation the ABC/ADRIQ varies the generator parameters in response to the demand for more or less signal from the detector, but the filter remains fixed. Each of the user-selectable fluoroscopy modes may have a different combination of pulse rate, EERD, generator control curve, and spectral filtration for each anatomical or procedural program. In addition, the system could be programmed to automatically change the filtration with change in SID.

IV.B.2. Seissl Method of Filter Selection

With the Seissl method, the ABC/ADRIQ plays an active role in the selection of one or more filters under a predetermined scheme. These actively selected filters are in addition to the nominal 2.5 mm Al total filtration which is required by regulatory agencies such as the FDA. While the exact scheme for determining which filters are selected is proprietary in nature, the task group has developed an experimental procedure to investigate just how the filters and other exposure parameters are varied. The procedure had been previously employed by Lin[51] to investigate the operation logic of a Siemens automatic dose control, and was subsequently modified by the task group for application with the various equipment designs studied. Fukuda et al.[52] also investigated the spectral shaping filter–equipped angiographic equipment. However, their focus was on skin dose evaluation as influenced by the variance of effective energy, and no discussion was given on the operational logic of automatic brightness (dose) control.

IV.C. Display of Filtration Utilized

Since the amount of spectral filtration is under program control, it is important to know how much filtration is in the beam for a given patient, protocol, beam geometry, and dose setting. Manufacturers initially did not provide a means for the user to know the type and amount of spectral filtration,[53] but today it is a requirement of the standards set forth by the FDA.[54] Figure 5 shows the various means of displaying the spectral filtration and other parameters by the manufacturers that were included in the study. Note that for these examples PW was displayed on the operator's control console only on the Siemens unit. For the GE Innova® 2100, PW indication was available on the image display monitor, but was not provided on any display by Shimadzu or Philips.

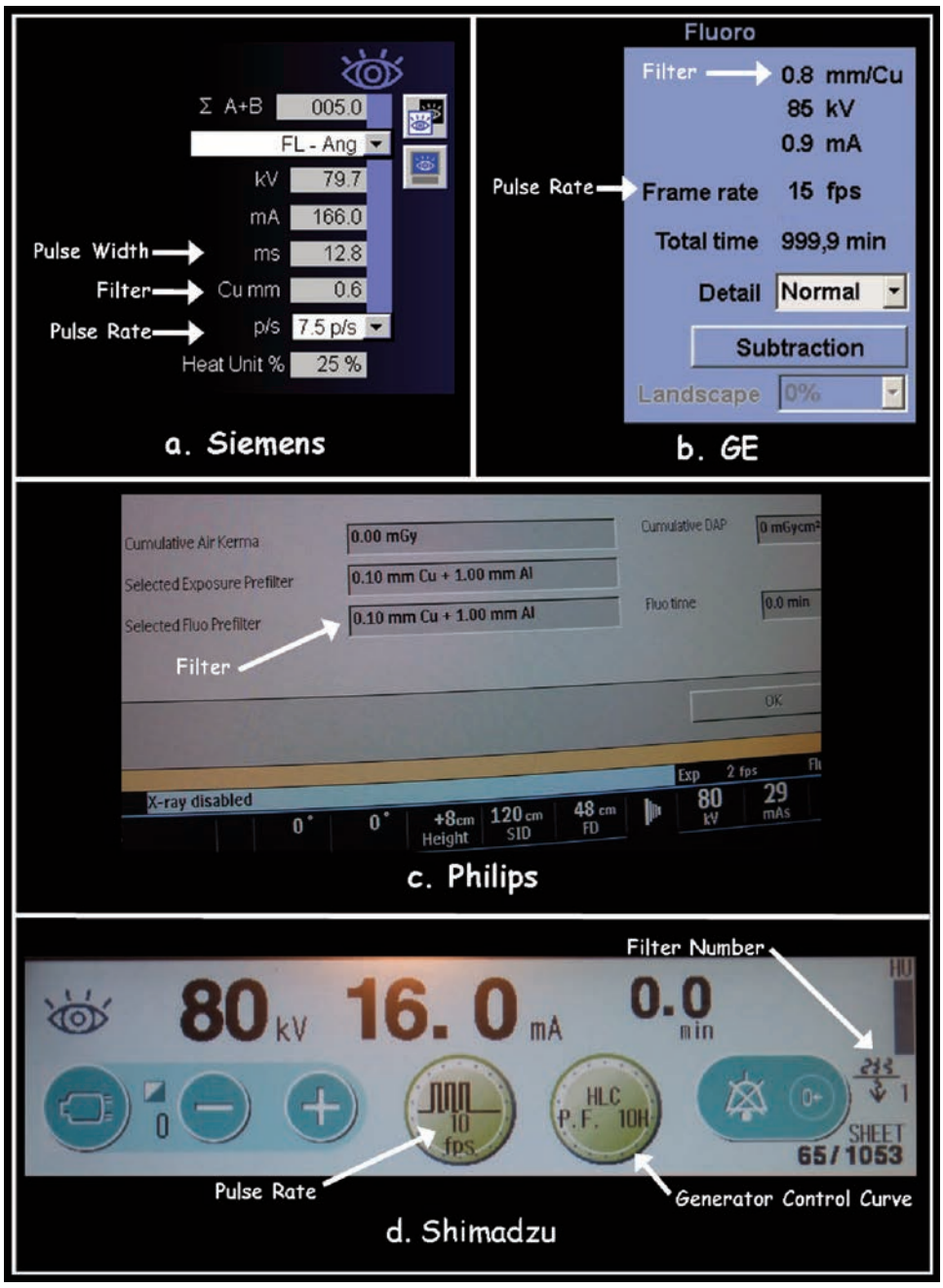

Figure 5. Display of the spectral filtration setting and other parameters on the operator's control modules of the imaging equipment included in this study. As evident from these images, there is no consistency in the way imaging parameters are displayed by the manufacturers.

V. The Automatic Brightness/Automatic Dose Rate Control

Before presenting the results obtained for the installed clinical systems evaluated by the task group, some background information on fluoroscopy systems in general should be reviewed. Much of this will consist of materials present in all medical physics textbooks but will also include some lesser-known features such as the currently utilized maximum radiation output compensation with change in SID.

V.A. Types of Automatic Control

Fluoroscopic x-ray systems make use of a set of rules (algorithms) that control the system's response to dynamic changes in imaging conditions. Usually these control algorithms maintain the absorbed energy fluence per pixel at the imaging detector's x-ray capture layer, resulting in a reasonably constant average signal level from the detector. The above statement is true for a given detector FOV. In general, manufacturers will change the nominal input exposure rate to the detector whenever the FOV is changed. The absorbed energy fluence per pixel is maintained by controlling the exposure parameters of the x-ray generator such that a constant, pre-defined detector signal level is achieved.

One of three methods are commonly employed: (1) a change in kVp with a fixed mA, (2) a change in mA with fixed kVp, or (3) a change in the kVp and the mA simultaneously. For some systems the exposure PW was varied adjunct to these three methods. The control of generator exposure factors to maintain a constant image receptor output signal is often called the Automatic Brightness Control (ABC), or Automatic Dose Rate Control (ADRC) mode of operation.

V.B. Automatic Gain Control

In all cases, it is either the light emitted from the output phosphor of the image intensifier, or the signal from the flat-panel detector that is utilized as the input signal for the ABC/ADRC. Since the x-ray generator response to a call for changes in technique can be relatively slow, AGC is utilized as an adjunct to the ABC/ADRC in order to compensate for changes in the signal strength at the input to the video chain.[55] In addition, the size of the aperture in the optical system transmitting the light from the output phosphor to the video camera can also be utilized as a means of maintaining a constant video signal level. In most cases a combination of ABC/ADRC control logic, AGC, and optical aperture modulation will be employed as a means of maintaining a reasonably constant video signal. The two most commonly employed methods of AGC, optical sampling and video sampling, will be further described below.

V.B.1. Optical Sampling AGC

The first method uses either an optical guide connected to a photomultiplier tube or, more common today, a solid-state photodiode array to sample the emitted light intensity. In the case of the photomultiplier, the detection window of the optics is adjusted to subtend a circle defining a percentage the output phosphor area. When a photodiode array is utilized, several pre-defined regions, either circular or rectangular, can be independently selected as the signal sensing region. In this way the signal can be sampled from either a central percentage area of the image or from one or more defined regions of the image.

V.B.2. Video Sampling AGC

The second method utilizes the video signal from the video camera for the ABC/ADRIQ input. In this case either the peak or the mean video signal within a selected region of interest (window) of the video image may be employed. This window is electronically selected and thus can be modified by the fluoroscopist to sample the video signal from a specific area of interest.

Both methods produce a signal that can be fed into the "Voltage Comparator," shown in Figure 6. The ABC/ADRIQ algorithm compares the input signal to the reference voltage. The reference voltage is established via a defined calibration procedure whereby a specific thickness of Cu is placed in the x-ray beam path and the EERD is monitored with a radiation dosimeter. As the reference voltage is varied, the generator parameters adjust and the EERD changes until a specified EERD is established under the calibration conditions. The target EERD will depend on the noise tolerance for the imaging task, the FOV selected, and the fluoroscopy pulse rate. Although the reference value is established using a dosimeter to measure the EERD, the ABC/ADRIQ does not necessarily maintain a constant EERD but rather reasonably constant absorbed energy fluence per pixel at the detector input. Because of the dependence of the detector absorption efficiency and energy conversion efficiency on the spectral energy distribution of the radiation, the established EERD using the Cu attenuator will not be the EERD achieved during patient imaging. It is rather a reference or calibration value achieved under specifically defined measurement conditions.

During clinical operation of the imaging system the reference values could, in some circumstances, be modified dynamically by the ABC/ADRIQ control logic. For example, to maintain image contrast for cases where the radiation attenuation is large, the system could be programmed to reduce the reference voltage in lieu of increasing the kVp beyond an established upper limit.

VI. Block Diagram of ABC/ADRIQ Circuit

This section describes the inner workings of ABC/ADRIQ circuitry so that the functions of the control logic may be fully appreciated. Depicted in Figure 6 is the overall schematic block diagram of a complete ABC/ADRIQ installed in typical angiographic imaging equipment.[56] In this figure an XRII system is used to demonstrate the functions of various controllers and subsystems. However, the entire box on the upper left corner of Figure 6 may be replaced by a flat-panel image receptor and its associated control logic/circuits. The descriptions given for an XRII-equipped system would still be valid for a flat-panel image receptor system with appropriate modifications. This is an artificially synthesized block diagram for the purpose of describing the ABC/ADRIQ. Some features may be preset while others are end-user selectable. The entire system could be illustrated by a simplified version as shown in Figure 7.

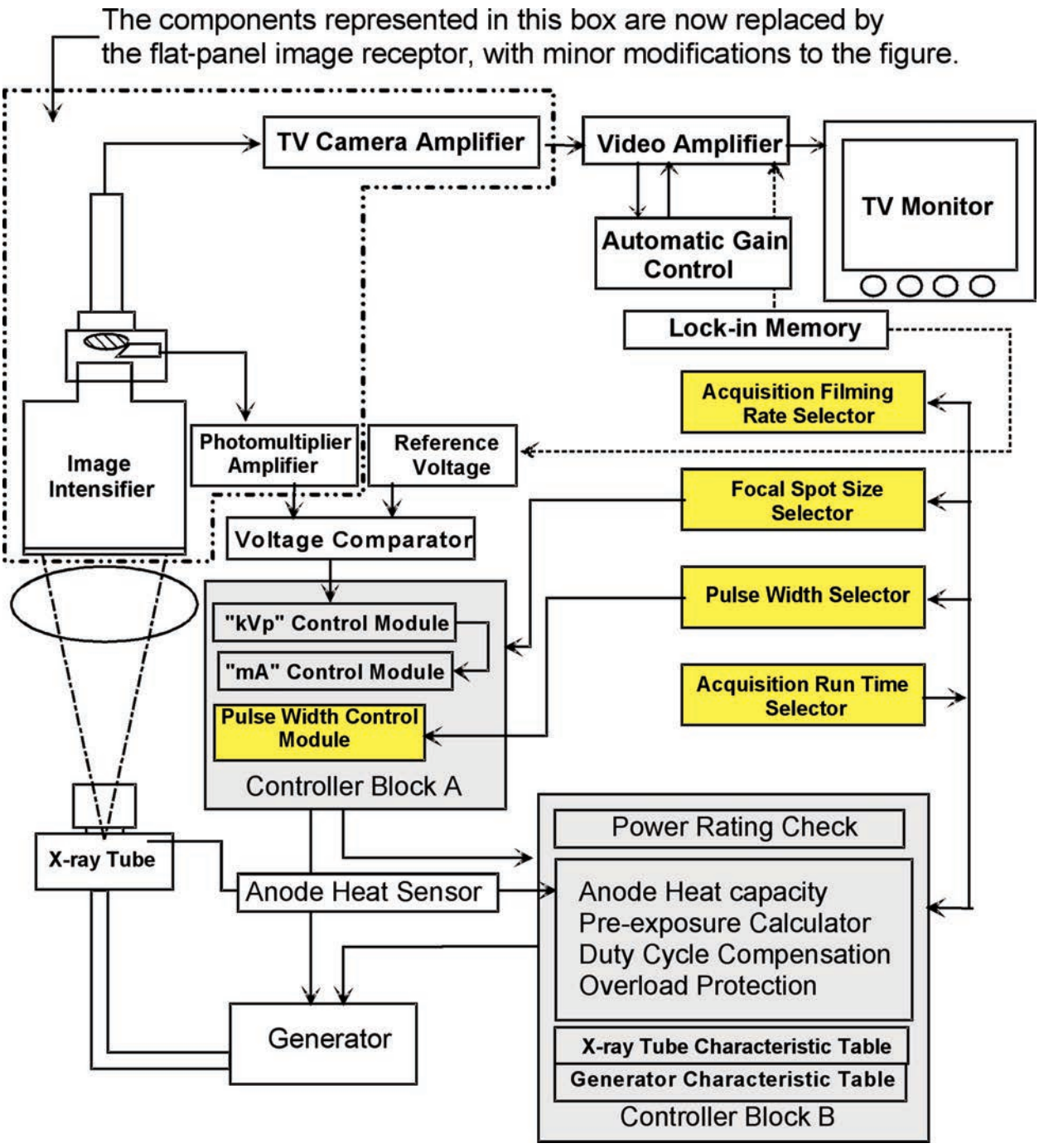

Figure 6. Typical schematic block diagram description of ABC/ADRIQ logic. (Adapted from reference 56.)

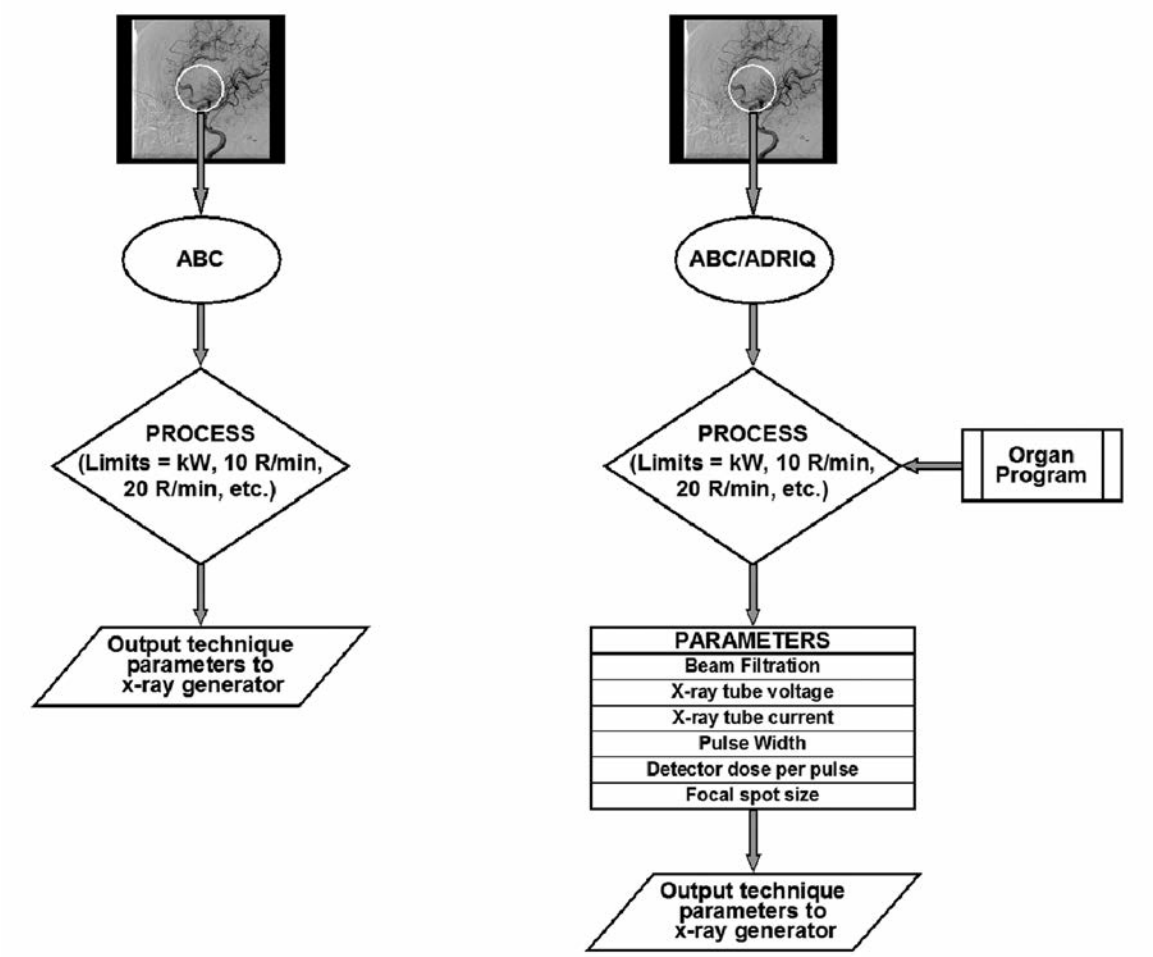

Figure 7. Flow diagrams for traditional ABC control logic (left), and modern ABC/ADRIQ control logic (right).

In the system depicted in Figure 7, the chart on the right shows imaging parameters that may be end-user selectable or preprogrammed in the control logic. In most modern fluoroscopic systems, these preprogrammed selections are referred to as "organ programs," and can be represented as shown. These imaging parameters may be preset to an initial start-up condition. For the fluoroscopy mode the initial settings might be pulsed fluoroscopy at 30 pulses per second (pps), 68 kVp, 10.5 mA_{rms}, and 7.5 ms PW; for the acquisition mode the initial settings could specify a cine frame rate of 30 fps, a digital subtraction angiography (DSA) frame rate of 4 fps, a digital serial acquisition frame rate of 2 fps, the small focal spot size, and a maximum run time of 10 seconds. The starting acquisition tube potential, tube current, and PW would also be established by the control logic of the ABC/ADRIQ, with these three parameters usually being derived from the previous fluoroscopy segment. These initial conditions are then dynamically modified as required to compensate for patient attenuation during the acquisition. In addition, Controller Block B of Figure 6 serves to ensure that any change in exposure parameters does not result in settings that would exceed the design limits of the x-ray generator or the x-ray tube, nor that the combination of generator parameters would result in radiation exposure rates that would exceed the regulatory limits. Included in Controller Block B are (1) an anode heat calculator which computes the anode heat accumulation and heat dissipation with incoming information of

tube potential, current, and exposure time, (2) the anode heat sensor which is incorporated into the x-ray tube housing assembly to monitor the anode heat buildup, (3) the x-ray tube heat loading characteristic table, (4) the generator power and duty cycle characteristics, and (5) various look-up tables and operational logic associated with radiological imaging parameters and their influence on the desired image quality. The level of sophistication of a given imaging system is to a large extent determined by what is in Controller Block B and the extent of the programmed operational logic.

To understand the simplest possible ABC/ADRIQ design for the fluoroscopy mode, one can treat most of the diagram on the right side of Figure 6 as a black box and concentrate on the Controller Block A for description and explanation. We can start by assuming that fluoroscopy has just been initiated and the pickup module, typically a photodiode array and signal preamplifier, begins to create a voltage proportional to that of the output phosphor brightness. This voltage is then fed into a voltage comparator shown just above the Controller Block A in the diagram. What happens next is dependent on the system design. In the case of the diagram shown in Controller Block A, it is based on a "kVp-primary" ABC/ADRIQ in which the tube potential functions as the primary control parameter. The following steps describe what the ABC/ADRIQ circuit is designed to do:

(1) As described previously, the initial pulsed fluoroscopy condition was set at 30 pps, 68 kVp, 10.5 mA_{rms}, and 7.5 ms PW. The actual mA generated during each x-ray pulse would be determined by dividing the mA_{rms} by the PW in seconds and then by the pulse rate. For the conditions described above, the actual mA would be (10.5 mA_{rms} / 0.0075 s / 30 pps) = 46.7 mA actual.

(2) The initial radiation passing through the patient and absorbed in the input phosphor of the XRII will generate a signal in the photodiode array.

(3) The signal from the photodiode array is compared against the preset reference voltage. This reference voltage is established via a calibration procedure and corresponds to a specified EERD obtained using the measurement conditions specified by the manufacturer.

(4) If the incoming signal to the Controller Block A differs from that determined by the reference voltage, the kVp control module would send a signal to the generator in order to appropriately adjust the tube potential.

(5) At the same time, this signal is fed to Controller Block B where various look-up tables are consulted by the ABC/ADRIQ. The function of the look-up tables is to ensure that the ABC/ADRIQ follows a pre-determined x-ray control curve or trajectory.[57]

(6) As the tube potential is being adjusted, the tube current and PW may also be changed in accordance with the selected trajectory, the x-ray tube anode heat storage characteristics, and the x-ray generator capabilities.

(7) New x-ray generator settings are then established (e.g., 72 kVp, 20 mA_{rms}, and 7.8 ms PW). These new settings then produce a photodiode signal that is equal to the reference voltage utilized by the voltage comparator, and a stable condition is achieved.

(8) The ABC/ADRIQ trajectories are designed to prioritize which parameters are modified and by how much they are allowed to change. Preference is generally given to keeping the kVp and PW constant, if possible, and therefore it is the tube current that will change first, followed by a change in PW (up to an established limit), and finally a change in kVp. The amount of spectral filtration can also change under program control as previously discussed.

(9) At this moment, if a cine acquisition run, DSA run, or digital serial run is initiated via the acquisition foot pedal, digital images would be acquired at the programmed frame rate, and the same ABC/ADRIQ system will serve to stabilize the detector output signal during the run. For each of these cases a different, calibrated reference voltage would be utilized and the radiation delivered to the detector per image frame would be much higher than that utilized for fluoroscopy. One might assume that logically all image frames would be recorded during acquisition and thus available for review via playback of the run. Unfortunately, this is not always the case, as for some equipment the user can choose a different image capture rate that is less than the x-ray exposure frame rate.

The operation of the imaging system described in (9) above is called "acquisition mode" to distinguish it from "fluoroscopy mode." In modern interventional angiography systems it can sometimes be difficult to discern from the program selection which mode is being utilized, since both produce short duration, pulsed exposures at a predetermined pulse rate. As stated above, the acquisition mode delivers a greater detector input dose per frame, but this distinction can generally not be determined by the operator. Also with modern equipment both fluoroscopy and acquisition frames can be stored for review during subsequent playback so storage/review is not a reliable means of distinguishing the two modes. One vendor simply labels the acquisition mode on its vascular C-arms with the word "Pulsed," which can easily be mistakenly interpreted to mean "Pulsed Fluoroscopy." The acquisition mode will not be described further in this report. The complexity of acquisition mode operation logic deserves a separate investigation and is beyond the scope of the current charge placed upon this task group.

While there are some boxes drawn in the diagram of Figure 6 that were not included in the above description, it is assumed that for a trained medical physicist, these components will be self explanatory. However, interested readers are invited to consult the references[58–60] listed at the end of this report if they desire a more in-depth description of these components. As previously mentioned, the functions of a flat-panel image receptor are designed to replace all of the functions of the image intensifier, optical distributor, video camera, and film cameras.[61] For flat-panel detectors the signal input to the ABC/ADRIQ is derived from sampling a pre-defined region of the detector. Two or more regions of different size, shape, and location are typically provided and are often user selectable either singly or in combination. Aside from the manner in which the signal is derived, for fluoroscopy imagers that utilize flat-panel detectors, the description given above for the operation of the ABC/ADRIQ control logic is valid without substantial changes.

VII. Task Group Field Evaluation of ABC/ADRIQ

VII.A. Angiography Systems Investigated

When TG-125 was established, it was intended to include most new angiography equipment available on the commercial market and from manufacturers known to the task group at the time. Due to the proprietary nature of the control logic design, none of the manufacturers were willing to share the explicit information on the generator control (trajectory) curves being utilized in their respective systems. In addition, the equipment available to the task group members was limited to (in alphabetical order) GE Healthcare (4 units), Philips Medical Systems (5 units), Shimadzu Medical USA (1 unit), and Siemens Medical Systems (12 units). The numbers in the parentheses correspond to the number of imaging systems evaluated. All equipment investigated was manufactured within the 3-year period from 2006 to 2008.

After preliminary analysis of the data collected, one representative system from each of the four manufacturers was selected to be included in this report. All of the selected systems utilized the most recent software version available at the time. The technical hardware parameters and information pertinent to this study are listed in Table 1. For consistency, the cardiac "coronary" angiogram program was selected for the data collection and the default settings were employed with the exception of the FOV. The selection of FOV for the flat-panel imagers tested was based on the *de facto* standard image intensifier size of 23 cm (9 inches), which have been installed in most cardiovascular angiography laboratories in the past decade. Although none of the systems used for data acquisition had a 23-cm FOV selection available, the one that was closest to 23 cm was chosen for the evaluation.

Although a wide variety of schemes for adjustment of the system operating conditions are available, a practical comparison of fluoroscopic systems can be made only for a finite set of

Table 1. Technical Hardware Parameters

Manufacturer Model	GE Innova 2100	Philips Allura Xper	Siemens Axiom Artis dFC	Shimadzu BRANSIST
Spectral Shaping Filter	Variable	0.1 mm Cu + 1 mm Al	Variable	Variable
Field of View (cm)	20	25	22	23
Focal Spot Sizes (mm)	0.3/0.6/1.0	0.5/0.8	0.3/0.6/1.0	0.5/0.8
Default Pulse Rate (pps)	15	15	15	10
Fluoroscopy Curve Label	Cardio IQ Plus	Fluoro Flavoure	70kV10RAF3kW	HLC H2
Fluoro Level Control	Normal	Dose Button II	Normal	Via Program
Focal Length, f_0 (cm)	100	100	105	100
Grid Ratio, r	15: 1	13:1	15:1	10:1
Line Density, N (lines/cm)	80	70	80	44

clearly defined algorithms. A representative set of control algorithms was chosen and the associated control logic was then investigated utilizing the methods described below.

VII.B. Experimental Arrangements

Depicted in Figure 8 is the experimental setup for the evaluation of fluoroscopic ABC/ADRIQ control logic of an angiography system. The SID was set to 120 cm or to the maximum SID available on the system being investigated. The tabletop–to–image receptor distance (TID) was kept at 40 to 43 cm (15.75 to 16.5 in.) so that there would be sufficient space to accommodate the ionization chamber and a total nominal phantom thickness of 38 to 41 cm (15 to16 in.). Due to the differences in the geometry of different systems, SID, TID, and maximum attenuator thickness had to be varied to some extent. A PMMA plastic phantom was employed to simulate the patient attenuation and varied from zero cm (zero in.) to 41 cm (16 in.) in increments of 2.54 cm (1 in.). As will be shown, in order to capture the discontinuity points of imaging parameters when the spectral shaping filter thickness was changed, increments of 0.635 cm (0.25 in.) were introduced to pinpoint the PMMA thickness where the ABC/ADRIQ produces a change in spectral filtration. The fluoroscopic imaging parameters kVp, mA, PW, Spectral Shaping Filter, and PAKR were recorded as a function of the attenuator thickness. Upon completion of the data acquisition, the fluoroscopic imaging parameters were plotted against the PMMA thickness. The graphs thus obtained reveal how the imaging system responded to changes in PMMA thickness, and thus how it would operate under clinical conditions. The SID of 120 cm may seem to be excessive, but considering that the C-arm positioner is frequently placed in a compounded angle, the SID of 120 cm is not necessarily unusual. It is important to note that no attempt was made to eliminate the effects of backscatter on the PAKR measurements. The support blocks shown in Figure 8 were utilized solely to support the PMMA in a position just slightly above the ioniza-

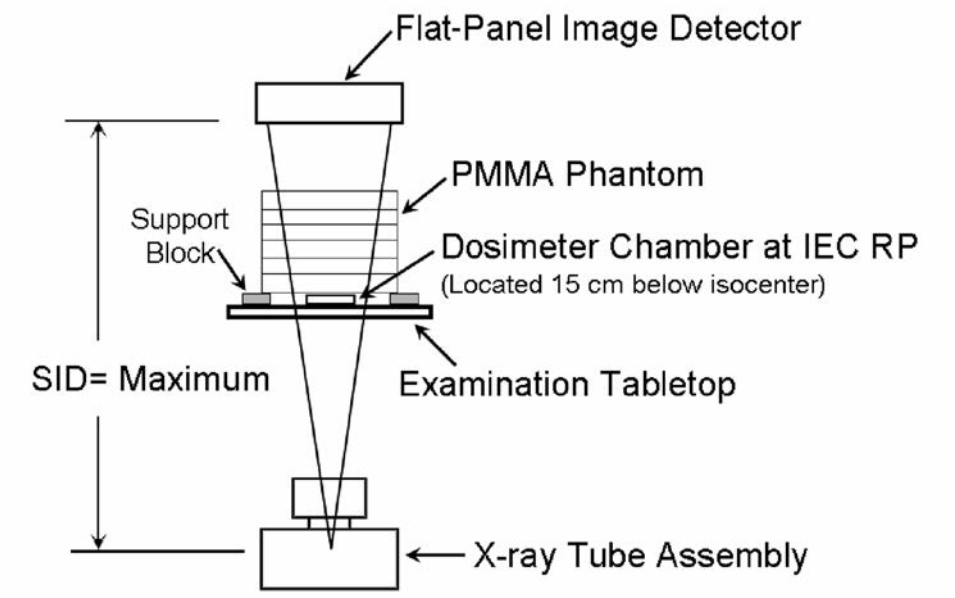

Figure 8. The experimental setup for the evaluation of fluoroscopic ABC/ADRIQ control logic of an angiography system.

tion chamber. The table mattress was removed. The reported PAKR will therefore not necessarily reflect that for a patient of equivalent thickness of PMMA due to the effects of table pad attenuation and backscatter. The focus of these measurements was on the operational logic of the imager, and was not intended specifically for patient dosimetry. Nevertheless the task group believes that the relative comparison of the reported PAKR values for different manufacturers is valid, since the geometry utilized was as identical as could be achieved in practice. Details of the measurement procedure utilized by the task group are provided in the appendix.

VII.C. Evaluation of Results

The generator control curves (kVp versus mA) for the four representative systems tested are shown in Figure 9. A single imaging system can have many such control curves, and these can take on different shapes based on the intended study application or anatomical protocol. For systems A and B on the left side of Figure 9, the spectral beam filtration switches automatically as the PMMA thickness is varied. For systems C and D on the right, the filtration associated with the selected program remains in place regardless of the beam attenuation. These functions are

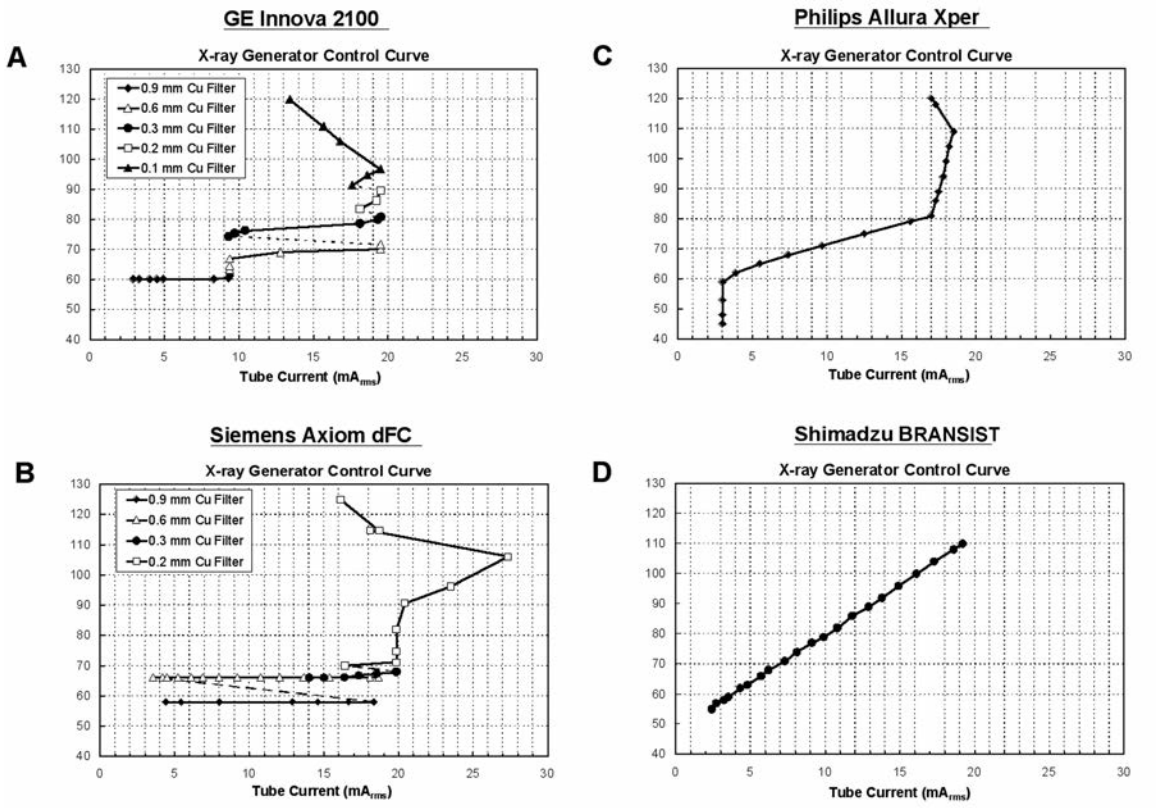

Figure 9. Generator control curves for the four representative units tested. A. GE Innova® 2100; B. Siemens dFC; C. Philips Allura Xper; and D. Shimadzu BRANSIST. The x-ray generator will follow the respective curve whenever the ABC/ADRIQ system demands more or less radiation in order to maintain a constant output signal from the detector. Many different control curves may be utilized, depending on the type of examination, focal spot size, and other factors.

described in more detail below for two angiography systems that utilize the Seissl method and for two systems that utilize the Program-Switched Method.

VII.C.1. Systems Using the Seissl Filter Method

Depicted in Figure 10 are the measurement results for the two systems, GE Innova® 2100 (left column) and Siemens Axiom Artis dFC (right column), that utilize the Seissl filter method. The graphs at the top of Figure 10, designated "A", show the tube potential and Cu filter thickness as functions of PMMA phantom thickness. Similarly, the middle graphs, "B", show the tube current and PW as functions of the PMMA thickness. The bottom graphs, "C", show the PAKR and the power loading versus the thickness of PMMA.

Let us follow the imaging parameter curves as the phantom thickness is increased in order to understand the operation of the control logic. Looking at charts A in both columns of Figure 10,

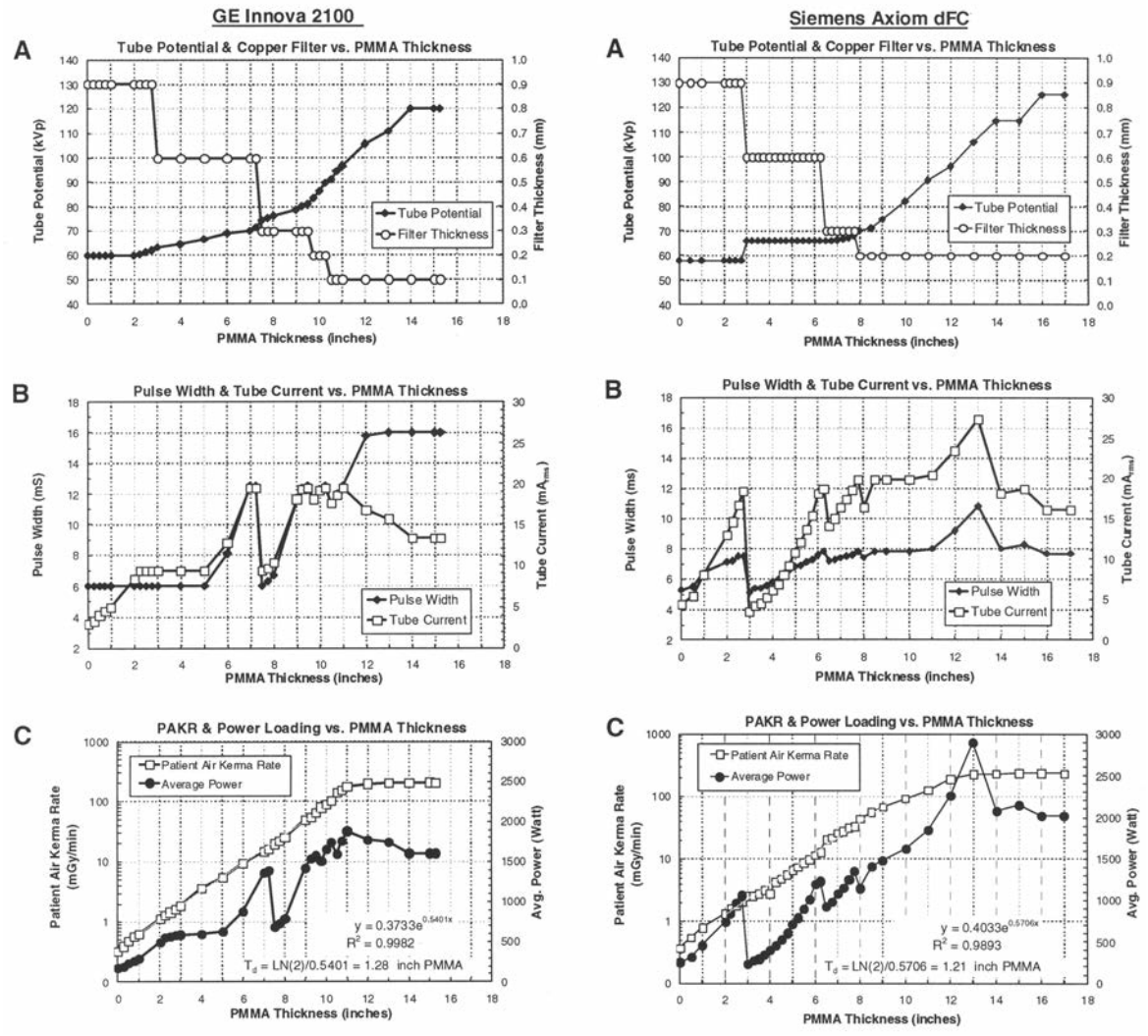

Figure 10. Various imaging parameters as a function of phantom thickness. Left: GE Innova® 2100. Right: Siemens Axiom dFC. A: Tube potential and Cu filter thickness; B: PW and tube current; and C: PAKR and Average Power. T_d is the calculated thickness of PMMA that doubles the PAKR.

it can be seen that the two vendors have slightly different approaches with regard to how the kVp changes with attenuator thickness. Below 2 in. PMMA neither vendor allows the kVp to drop as the attenuator thickness decreases. However, between 3 in. and 8 in. GE allows the kVp to increase whereas Siemens holds the kVp relatively constant. For both vendors the filter changes only in incremental steps, but each vendor uses a slightly different number of steps and minimum filter thickness. In general, the minimum thickness of spectral filtration will be factory set, but there may be means provided for service to program the minimum thickness desired for specific applications such as electrophysiology (EP) or pediatric studies. To further understand the manner in which the ABC/ADRIQ logic functions, we shall examine the GE Innova® 2100 curves more closely. As seen from the graphs in the left column of Figure 10, the GE Innova® 2100 ABC/ADRIQ logic operates as follows:

(1) Initial Conditions (No attenuator)
   a. Filter 0.9 mm Cu.
   b. Tube Potential 60 kVp.
   c. Tube Current 3 mA_{rms}.
   d. PW 6 ms.

(2) PMMA thickness 0–2 in.
   a. Filter remains constant at 0.9 mm Cu.
   b. Tube Potential remains constant at 60 kVp.
   c. Tube Current increases from 3 mA_{rms} to 9 mA_{rms}.
   d. PW remains constant at 6 ms.

(3) PMMA thickness 2–3 in.
   a. Filter remains constant at 0.9 mm Cu.
   b. Tube Potential gradually increases from 60 to 63 kVp.
   c. Tube Current remains constant at 9 mA_{rms}.
   d. PW remains constant at 6 ms.

(4) PMMA thickness 3–5 in.
   a. Filter drops to and remains constant at 0.6 mm Cu.
   b. Tube Potential gradually increases from 63 to 67 kVp.
   c. Tube Current remains constant at 9 mA_{rms}.
   d. PW remains constant at 6 ms.

(5) PMMA thickness 5–7.5 in.
   a. Filter remains constant at 0.6 mm Cu.
   b. Tube Potential gradually increases from 67 to 75 kVp.
   c. Tube Current rapidly increases from 9 to 20 mA_{rms}.
   d. PW rapidly increases from 6 to 12.5 ms.

(6) PMMA thickness 7.5–9.5 in.
   a. Filter drops to and remains constant at 0.3 mm Cu.
   b. Tube Potential gradually increases from 75 to 81 kVp.
   c. Tube Current drops back to 9 mA_{rms}, then rapidly increases from 9 to 20 mA_{rms}.
   d. PW drops back to 6 ms, then rapidly increases from 6 to 12.5 ms.

(7) PMMA thickness 9.5–10.5 in.
   a. Filter drops to and remains constant at 0.2 mm Cu.
   b. Tube Potential gradually increases from 81 to 91 kVp.
   c. Tube Current drops to 18 mA_{rms}, then rapidly increases from 18 to 20 mA_{rms}.
   d. PW drops to 11.5 ms, then rapidly increases from 11.5 to 12.5 ms.

(8) PMMA thickness 10.5–14 in.
   a. Filter drops to and remains constant at 0.1 mm Cu.
   b. Tube Potential gradually increases from 91 to 120 kVp.
   c. Tube Current drops to 18 mA_{rms}, then rapidly increases from 18 to 20 mA_{rms}, followed by a rapid decrease from 20 to 13 mA_{rms}.
   d. PW drops to 11.5 ms, then rapidly increases from 11.5 to 16 ms (at 12 in. PMMA), then remains constant at 16 ms between 12 and 14 in. PMMA.

(9) PMMA thickness >14 in.
   a. Filter remains constant at 0.1 mm Cu.
   b. Tube Potential remains constant at 120 kVp.
   c. Tube Current remains constant at 13 mA_{rms}.
   d. PW remains constant at 16 ms.

Further analysis of how the imaging parameters changed as the PMMA thickness increased revealed additional insights into the operation of the control logic. As already stated, the kVp was never allowed to drop below 60 kVp, even when the PMMA thickness approached zero. This condition, along with the fact that the maximum spectral filtration was present for PMMA thicknesses below 3 in., should serve to greatly lower the skin dose during neonatal fluoroscopy as compared to that which would have occurred with systems using only minimum allowed filtration and having generator control curves that continued to lower the kVp as the attenuator thickness was reduced.

It was also interesting to note that, at least up to 11 inches PMMA, the PAKR increases exponentially with increase in PMMA thickness, and without any sudden discontinuities, even at the PMMA thicknesses where the filter was abruptly changed. The result is a linear relationship between the PAKR and the PMMA thickness when plotted on a semi-logarithmic graph as shown in graphs C of Figure 10. This relationship allows calculation of the incremental PMMA thickness, T_d, that would double the PAKR. Note that above 12 in. of PMMA the PAKR remains constant due to the regulatory limits imposed by the FDA. The values for the PAKR limit shown on the graphs do not match the limits imposed by the FDA due to the fact that (1) the measurement geometry used by the task group did not conform to the FDA-defined measurement geometry, and (2) the presence of scattered radiation from the PMMA.

Regarding PW, it is evident from the graphs that for PMMA thicknesses from 0 to 11 in., the PW was allowed to vary only in the range from 6 to 12.5 ms, and for PMMA thicknesses of 12 in. or more, the PW was held constant at 16 ms. It can be assumed that the lower limit to the PW was imposed in order to keep the power requirements within the ratings of the x-ray generator and the x-ray tube, and the upper limit to the PW was imposed as a means of preserving temporal resolution.

In the same manner as used above to describe the operational logic of the GE Innova® 2100, the ABC/ADRIQ logic of the Siemens Axiom dFC can be discerned. The principal difference between these two systems is the fact that for the Siemens imager the changes in kVp, mA, and PW correlate much more closely to the associated filter thickness changes. The similarity of these two manufacturers in the ABC/ADRIQ logic designs can be attributed to the fact that both manufacturers utilize the same collimator assembly manufactured by Siemens. Observed differences are due primarily to the engineering design (e.g., GE reduced the added filtration to 0.1 mm Cu filter for some fluoroscopy modes, whereas Siemens did not allow less than 0.2 mm Cu during fluoroscopy), the capabilities of the generator, and the specifications of the x-ray tube. It should be noted that in graphs B of Fgure 10 the values of tube current are root-mean-square (mA_{rms}) values. This is also the case for the display of mA on the GE control console. However, Siemens displays the average of the tube current present during each x-ray pulse. Thus for the Siemens chart the per-pulse average mA value recorded from the display console is converted to the time average value of mA_{rms}.

VII.C.2. Systems Using the Programmable Filter Method

VII.C.2(i). Philips Allura Xper System

The Philips Allura Xper system employs the design concept associated with the program-switched filter method. Once a clinical program is selected at the control console and the fluoroscopy dose level at the examination tableside controller is selected, a particular filter is switched into the x-ray beam path. Thus the type and thickness of filtration is determined by the program selected and no variation is permissible via the ABC/ADRIQ control as the patient attenuation is varied. The filter arrangement for the unit investigated was set to 0.1 mm Cu plus 1.0 mm Al. This filtration is in addition to the nominal 2.5 mm Al total filtration that is required by regulatory requirements.

Figure 11 shows graphs of the test data for the Philips Allura Xper and the Shimadzu BRANSIST. Graphs A are for the fluoroscopic Tube Potential (kVp), graphs B are for the PW and Tube Current (mA_{rms}), and graphs C are for the PAKR and average power loading. For these two systems the spectral shaping filter is fixed, as mentioned previously. Neither of these systems displays the PW to the operator. However, for the Philips Allura Xper system the PW data were collected by attaching a dual-trace storage oscilloscope at the mA-test point in the generator cabinet. Normally, the kVp-test point would be accessed for measurement of tube potential as well as for PW information. However, the specific model of generator utilized by the system does not have a kVp-test point.

With a fixed filter there are no sudden changes in primary beam intensity that would otherwise be caused by the changing spectral shaping filter. Therefore the PAKR will exponentially increase as the tube potential and the tube current simultaneously increase with phantom thickness. This increase in PAKR occurs up to the thickness that produces either the maximum allowed PAKR, or the maximum power load for the system.

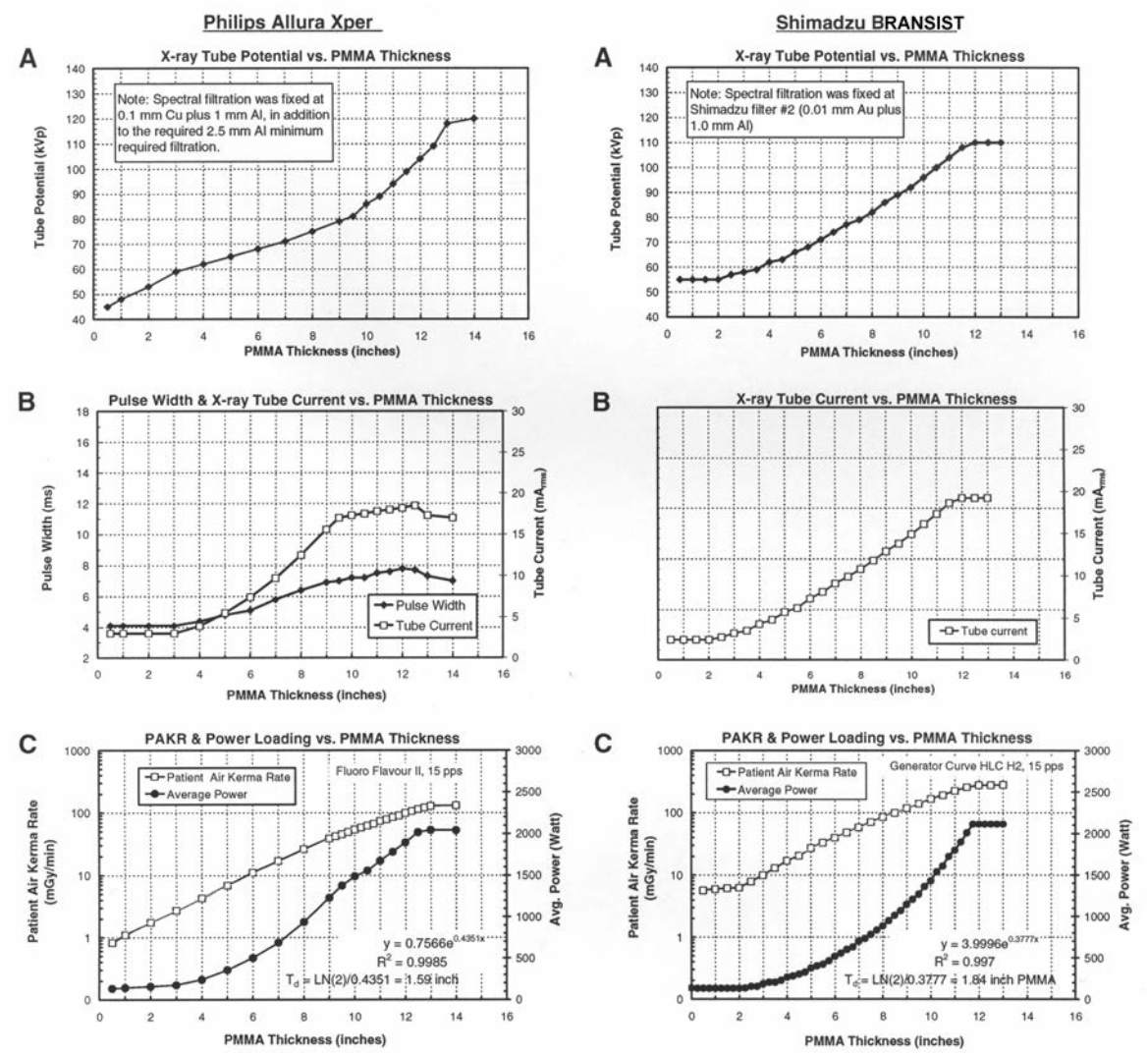

Figure 11. Various imaging parameters as a function of phantom thickness. Left: Philips Allura Xper; Right: Shimadzu BRANSIST. A: Tube potential; B: PW and tube current; C: PAKR and Average Power. Neither Philips nor Shimadzu indicated the PW. The Philips PW data were obtained via a storage oscilloscope. T_d is the calculated thickness of PMMA that doubles the PAKR.

VII.C.2(ii). Shimadzu BRANSIST Cardiovascular

The Shimadzu BRANSIST is a dedicated cardiovascular imaging system with a direct-capture flat-panel detector. The BRANSIST utilizes four composite filters, all located on a motorized disc inside the collimator. Selection of filtration is via program control. A specific filter is assigned to each user-selectable program and is also assigned according to the SID. That is, for SID values less than or equal to 96 cm, a given filter is associated with each anatomical program, and for each dose mode in that program. For SID values equal to or greater than 97 cm, the filter could be the same or could change according to the factory program (see Table 2 and Table 3). In addition to the programmed selection of spectral filtration, Shimadzu provides the user with the ability to manually select filter #4 and, when this filter is manually selected, it remains in the beam independent of the SID. The filtration did not change with patient size and

Table 2. Shimadzu BRANSIST Filters and Their Programmed Utilization

Filter	Material	Thickness (mm)	Fluoro Mode	Acq Mode	HVL (mm Al at 80 kVp)	Filter Utilization
#1	Al Cu	2 0.1	X	X	4.99	Whenever the SID is less than or equal to 96 cm, filter #1 is utilized for all 10 pps/H fluoro modes and selected 15 pps fluoro modes. It is also used for all OneShot Acquisition at any SID.
#2	Al Au	1 0.01	X	X	3.83	Whenever the SID exceeds 96 cm, filter #2 replaces the above-listed filter #1 settings for fluoro. Filter #2 is the only one utilized for all radiographic modes, except when the "P" (upper left button on the collimator control box) is selected, or for Single Shot as described above.
#3	Al Cu	1.5 0.3	X	NA	5.9	Filter #3 is utilized for selected 15 pps fluoro modes and, when utilized, it is in place for all SID settings.
#4	Al Cu	1.5 0.6	X	NA	7.5	Filter #4 is used for all Head and Peri fluoro protocols except the 10 pps/H. It is also utilized for selected Cardiac and Ablation fluoro protocols. It is not utilized for any Abdomen fluoro protocols.

therefore would be classified as the program-control method. Figure 12 shows the measured PAKR and EERD as a function of PMMA attenuator thickness for the Shimadzu BRANSIST. It should be noted that the EERD would not normally be measured with PMMA, but since this material is often used to simulate patient attenuation, it is instructive to see how the PAKR and EERD varies with changes in PMMA thickness. An exponential fit to the straightline portion of the PAKR plot reveals that the x-ray spectra was slightly harder with the 15 pps program (T_d = 1.72 in. acrylic) versus the 30 pps program (T_d = 1.64 in. acrylic), which uses a different generator control curve. Note also that the PAKR was much lower for the 30 pps program. This result was not expected and led to investigation of the exposure rate values for all of the selectable programs (Figure 13). The different x-ray control curves utilized by Shimadzu, along with the factory-set dose program, gave rise to the unexpected result that the 30 pps protocol produces a lower PAKR than that obtained with the 15 pps protocol. Of particular concern was that the

Table 3. Shimadzu BRANSIST Filter Changeover Program

Summary: For fluoroscopy, the filter automatically changes when the SID changes from 96 cm to 97 cm.
For Acquisition the filter does not change until the prep switch is pushed and does not change with SID

Fluoroscopy Modes

Cardiac Modes

Selection	Filter Number SID (cm) 96	97
10pps/H	1	2
15pps	3	3
30pps/H	4	4
30pps	4	4
15pps/H	1	2
15pps/H(-)	4	4
15pps(-)	4	4

Head Modes

Selection	Filter Number SID (cm) 96	97
15pps/H IVR	4	4
MAP 15pps/H	4	4
S.I. 15pps/H	4	4
15pps/H	4	4
15pps IVR	4	4
S,I. 15pps	4	4
15pps	4	4
10pps/H	1	2

Peri Modes

Selection	Filter Number SID (cm) 96	97
15pps/H IVR	4	4
MAP 15pps/H	4	4
S.I. 15pps/H	4	4
15pps/H	4	4
15pps IVR	4	4
S,I. 15pps	4	4
15pps	4	4
10pps/H	1	2

Abd Modes

Selection	Filter Number SID (cm) 96	97
15pps/H IVR	1	2
MAP 15pps/H	1	2
S.I. 15pps/H	1	2
15pps/H	1	2
15pps IVR	3	3
S.I. 15pps	3	3
15pps	3	3
10pps/H	1	2

Acquisition Modes

Cardiac Modes

Selection	Filter Number SID (cm) 96	97
CAG[15F-10S]	2	2
LVG[30f-15s]	2	2
AOG[15f-30s]	2	2
CAG[30f-15s]	2	2

Head Modes

Selection	Filter Number SID (cm) 96	97
DSA[3f-20s]	2	2
DSA[2f-30s]	2	2
DSA[7f-30s]	2	2
DSA[5f-40s]	2	2
RSM[15f-20s]	2	2

Peri Modes

Selection	Filter Number SID (cm) 96	97
RSM[15f-30s]	2	2
DSA[3f-20s]	2	2
DA[15f-30s]	2	2
RSM[15f-15s]	2	2
DSA[2f-30s]	2	2
DSA[7f-30s]	2	2
DSA[5f-40s]	2	2

Abd Modes

Selection	Filter Number SID (cm) 96	97
DSA[3f-20s]	2	2
DSA[2f-30s]	2	2
DSA[7f-30s]	2	2
DSA[5f-40s]	2	2
RSM[15f-20s]	2	2
OneShot	1	1

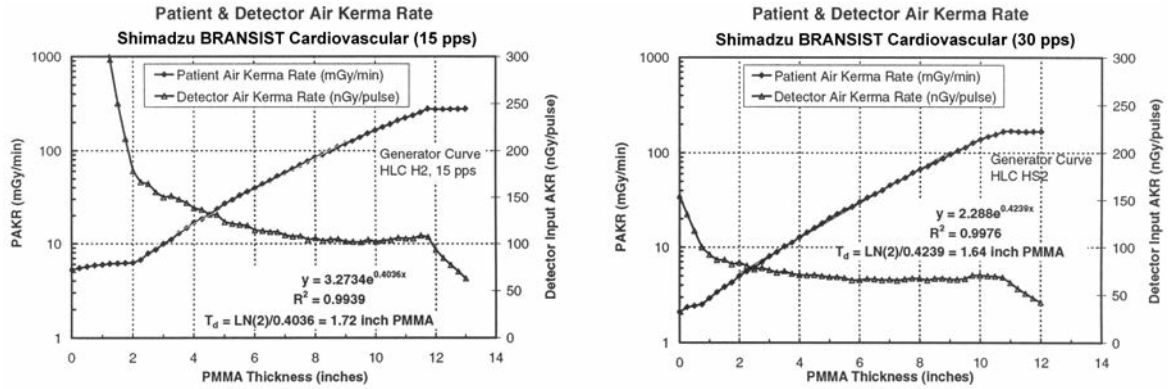

Figure 12. Shimadzu BRANSIST PAKR and detector entrance AKR versus PMMA thickness. Left: Fluoroscopy at 15 pps. Right: Fluoroscopy at 30 pps. T_d is the calculated thickness of PMMA that doubles the PAKR.

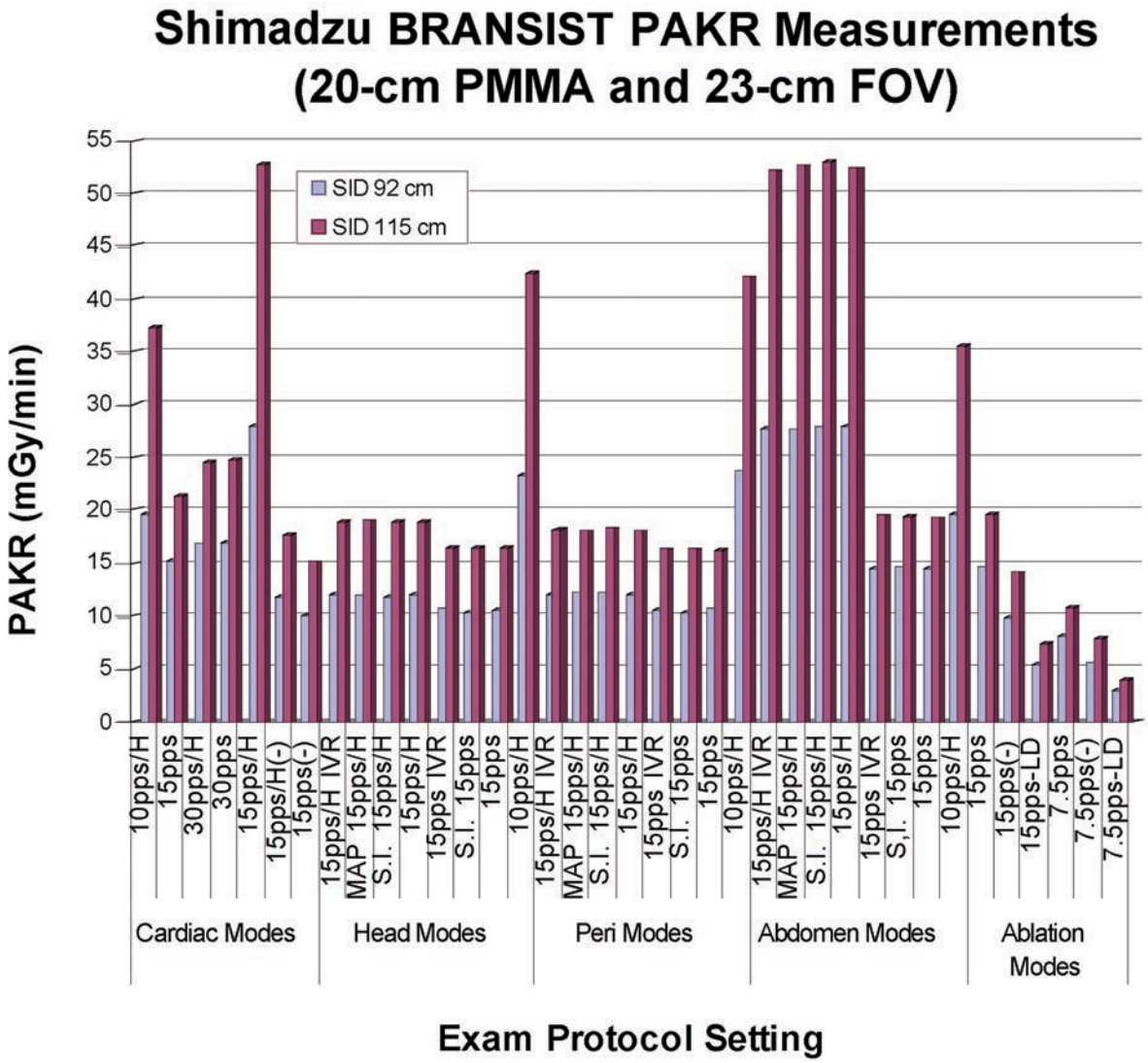

Figure 13. PAKR measurements with two different SID settings. Data acquired using 20 cm PMMA, with the 23-cm FOV, and for all Shimadzu BRANSIST protocol settings. Note that for all 10 pps/H settings the dose rates are greater than for any of the 15 pps settings; and that the 15 pps/H settings deliver a greater dose rate than the 30 pps/H settings.

highest PAKR occurred when the 10 pps/H setting was selected. Of equal concern was the observation that in general the 15 pps/H PAKR values were greater than those for the 30 pps/H settings. This is contradictory to the normal understanding (and *de facto* standard) that lower fluoroscopy pulse rates result in lower patient dose rates. For this machine, and with the exception of the ablation modes, the lowest selectable pulse rates produce the highest patient dose rates. Furthermore, it was revealed that the 10 pps/H mode was the default setting selected automatically on start-up of the system. Since most radiation safety programs teach that lower pulse rates produce lower patient doses, the user must be cognizant that the Shimadzu BRANSIST does not conform to this norm.

VII.C.2(iii). Toshiba Infinix CF-i and Infinix VF-i

Toshiba manufactures 10 different types of gantry systems, and with these systems there are two collimator models employed. The angiography systems Infinix CF-i and Infinix VF-i employ collimators BLA-800C and BLA-900A, respectively. The BLA-800C system was equipped with the following filters: 0.2 mm Cu, 0.3 mm Cu, and 1.8 mm Al; while the BLA-900A included: 0.2 mm Cu, 0.3 mm Cu, 0.5 mm Cu, and 1.8 mm Al.[62] The ABC/ADRIQ control logic of Toshiba cardiovascular equipment is believed to function in a manner similar to the Philips angiographic equipment. However TG-125 was unable to gain access to a Toshiba angiography system to conduct a comprehensive evaluation. Hence, no additional data can be provided.

VII.C.2(iv). Hitachi Medical Systems

Hitachi Medical Systems was unable to provide potential angiography sites for TG-125 to perform evaluation and, therefore, no data are presented here.

VIII. Problem with Lack of Appropriate Standard Beam Qualities

In the process of collecting data for the TG-125 report, a lack of appropriate standard beam qualities for highly filtered fluoroscopic beams has been recognized. This problem is being pointed out in this report so that positive actions may be taken by appropriate organizations and authorities to remedy the situation. Specifically, there is a lack of standard beam qualities available for calibration of ionization chambers for the beam quality (spectra) being employed in clinical fluoroscopy systems designed for angiographic imaging.

VIII.A. Measured Fluoroscopic X-Ray Beam Quality

Depicted in Figure 14 is the fluoroscopic radiation beam quality, in terms of HVL, obtained from the Siemens angiography equipment. The HVL data were obtained under the service mode that allowed manual selection of kVp and mA at a fixed exposure time of 100 ms. In this mode, there was no ABC/ADRIQ intervention. As seen in Figure 14, the combination of thickest Cu filters (0.6, 0.9 mm Cu) with low tube potentials (60 to 75 kVp) yielded beam quality in the range of 6 to 9 mm Al HVL. Calibration of ionization chambers for this beam quality cannot be found in any national calibration laboratories.

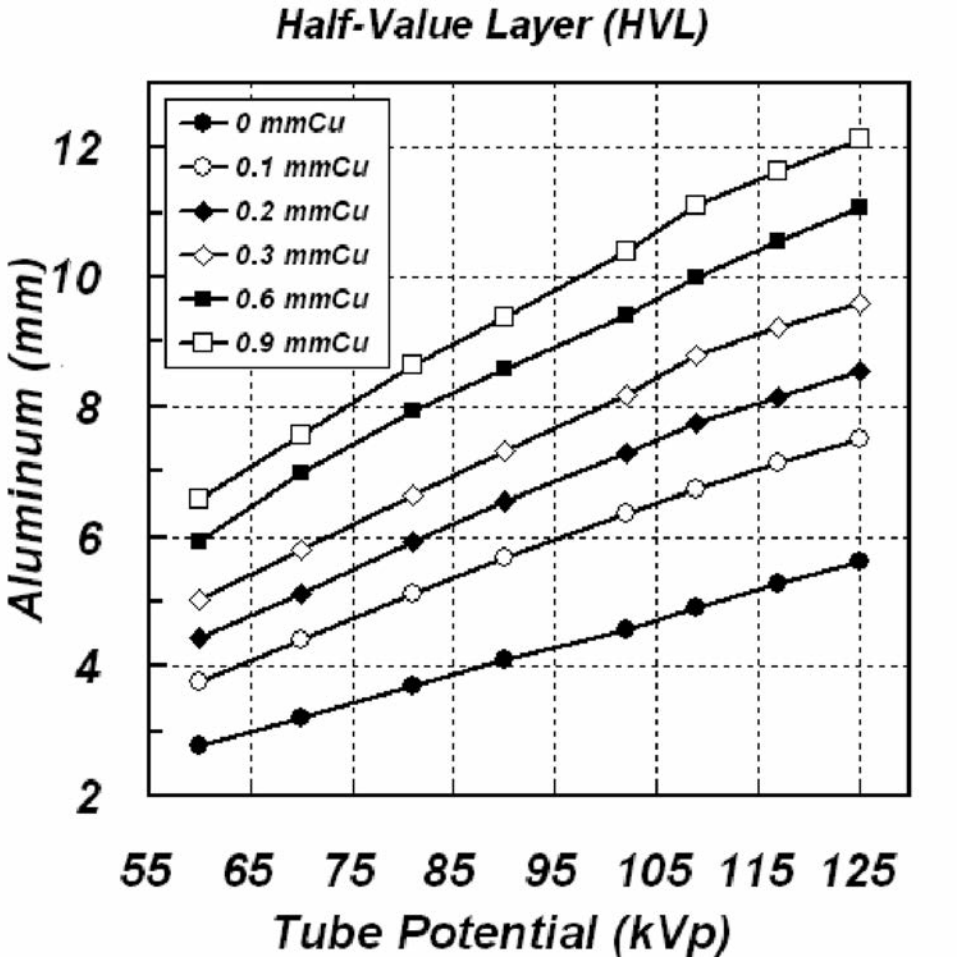

Figure 14. Typical radiation beam quality (HVL) for angiography systems utilizing various thicknesses of Cu spectral beam filtration.

VIII.B. The Beam Quality Available for Calibration

The instrumentation utilized for measuring fluoroscopic air kerma and AKR include air-equivalent ionization chambers and energy-compensated solid-state detectors. The calibration of such instruments should be ultimately traceable to the National Institute of Standards and Technology (NIST),[63] or equivalent national calibration standards. International Electrotechnical Commission (IEC) publication 61267 (ed. 2.0, 2005), "Medical Diagnostic X-ray Equipment - Radiation Conditions for Use in the Determination of Characteristics"[64] describes the set of calibration beams available in most national laboratories and are reproduced here in Table 4 and Table 5 with permission from the IEC.

VIII.C. The Mismatch of Beam Quality for Dosimetry

Most diagnostic instruments used for measuring patient/phantom skin dose are calibrated using the RQR[†] series of beams. Instruments used for measuring image-receptor input dose are

[†]RQR: Radiation Qualities in Radiation beams emerging from the x-ray tube assembly.

Table 4. Characterization of Standard Radiation Qualities RQR 2 to RQR 10

Standard Radiation Quality	X-Ray Tube Voltage (kVp)	Homogeneity Coefficients	Nominal First HVL in Thickness of Aluminum (mm)
RQR 2	40	0.81	1.42
RQR 3	50	0.76	1.78
RQR 4	60	0.74	2.19
RQR 5	70	0.71	2.58
RQR 6	80	0.69	3.01
RQR 7	90	0.68	3.48
RQR 8	100	0.68	3.97
RQR 9	120	0.68	5.00
RQR 10	150	0.72	6.57

Table 5. Characterization of Standard Radiation Qualities RQA 2 to RQA 10

Standard Radiation Quality	X-Ray Tube Voltage (kVp)	Added Filter Thickness of Aluminum (mm)	Nominal First HVL in Thickness of Aluminum (mm)
RQA 2	40	4	2.2
RQA 3	50	10	3.8
RQA 4	60	16	5.4
RQA 5	70	21	6.8
RQA 6	80	26	8.2
RQA 7	90	30	9.2
RQA 8	100	34	10.1
RQA 9	120	40	11.6
RQA 10	150	45	13.3

typically calibrated using the RQA[†] series of beams. According to the IEC, the RQR series was obtained by changing the voltage applied to a tungsten (W) target x-ray tube filtered with a few millimeters of Al. The RQA series was obtained by adding the specified additional Al at each beam quality. As shown in Table 4, in each series the HVL increases with x-ray tube voltage.

Modern interventional fluoroscopic equipment incorporate beam filters with an atomic number equal to or higher than that of Al, with Cu being the most common. The systems described in this report were all filtered with combinations of Cu and Al, with two systems also utilizing a high atomic number material. As described elsewhere in this report, the filter may either be programmed to the selected anatomical protocol and fluoroscopic dose setting, or determined under dynamic control of the ABC/ADRIQ. Typically, systems of the latter type reduce the thickness of spectral filters as the patient/phantom thickness is increased. This was evident in the graphs A of Figure 10. Representative data for the kVp and filter thickness combinations selected during fluoroscopy and acquisition are shown in the bar graphs of Figure 15. The thickness of Cu filters (mm Cu) inserted by the ABC/ADRIQ for each phantom size is shown on the right ordinate. Notice that the tube potential increases while the Cu filter thickness decreases as the PMMA phantom thickness increases.

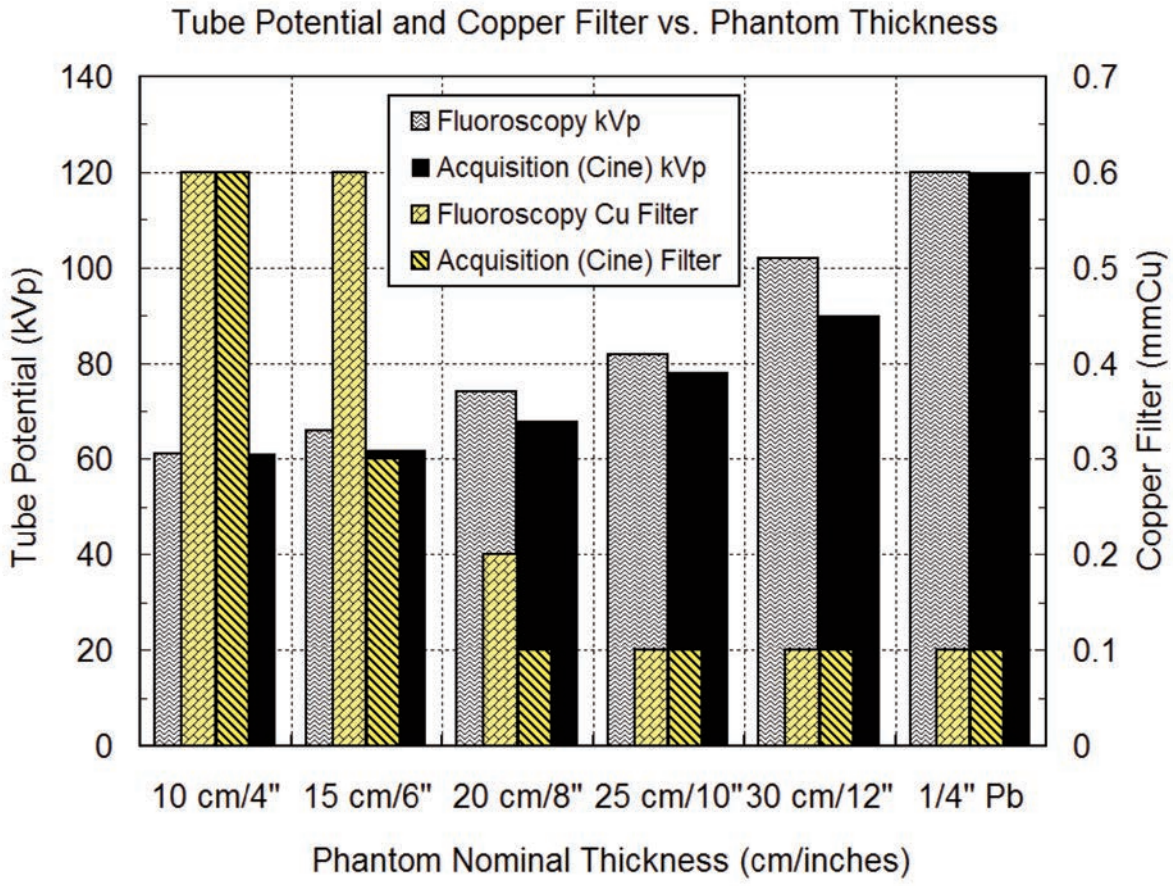

Figure 15. Sample of the relationships between phantom thickness, x-ray tube potential, and Cu filtration for a typical modern angiography system.

[†]RQA: Radiation Qualities based on a phantom made up of an Aluminum added filter.

Currently, the national laboratories are in the process of developing a set of calibration beams suitable for interventional fluoroscopic systems. Until these beams are available, the medical physics community needs to take appropriate care in the selection of dose instruments to avoid having the measurements made on such systems confounded by spectral effects.

IX. Limitations of the Report

For the reasons listed below, the information contained in this report will have limitations as to its accuracy and its application to any specific angiographic system.

(1) The development and progress of angiography imaging technology is so fast that the information presented in this report might become obsolete within the next 3 to 5 years.

(2) The data collected and the analysis provided are based on newly manufactured equipment having the latest software versions as of February 2008. While newer versions of software have been implemented since that date, the basic operations remain the same to this date (February 2012).

(3) This report should be reviewed as a "snapshot" of equipment design and functionality for angiography systems available on the commercial market and accessible by TG-125 during the time period that the information and data were obtained.

(4) While image quality optimization was part of the initial charge, the task group members believe that this subject was sufficiently extensive that it deserves to be addressed separately, perhaps by a new task group.

Although there were more than 20 angiography systems investigated by this task group, the data presented in this report were derived from just four systems: one each from GE Healthcare, Philips Healthcare, Shimadzu Medical Systems USA, and Siemens Medical Solutions, all of which were installed in the institutions of the task group members. While it is difficult to predict the technology of the future, it is believed that the use of thick spectral filtration and the programmed control of multiple imaging parameters will continue to be utilized by the manufacturers of interventional angiography systems for many years to come.

X. Conclusion and Discussion

Two of the three original charges assigned to TG-125, namely;

(1) Explore and investigate the functionality of fluoroscopic automatic brightness (dose) control logic (ABC/ADRIQ) in modern angiography systems, and

(2) Describe the manner in which imaging parameters are programmed to work with changing spectral filter thickness

have been accomplished. It is hoped that the information provided in this report will enhance the practicing medical physicists' working knowledge, and will thus facilitate their ability to meet the National Council on Radiation Protection and Measurements (NCRP) recommendation that

"Interventionalists and qualified physicists should participate in the process for purchase and configuration of new fluoroscopes and fluoroscopy facilities."[65]

It should be clear that the beam quality of modern cardiovascular angiography imaging systems can be quite different from traditional fluoroscopy equipment. On the other hand, new installations of traditional fluoroscopy equipment designed for upper-lower gastrointestinal examinations, endoscopy, gastroenterology, and pain management have been found to also employ added spectral filtration to reduce patient exposure, or PAK.[66] The work of TG-125 has revealed a lack of standardization of radiation measurement instrument calibration at the beam qualities being employed in modern image-guided interventional equipment. Additional work is needed in order to understand the impact of beam quality on radiation measurement accuracy and to determine if a new beam quality standard should be made available by calibration laboratories for radiation detectors used to measure fluoroscopic dose.

Since the power train (x-ray generator control, transformer, and exposure switching mechanism) of traditional fluoroscopy equipment is generally lower in power ratings than that of fluoroscopy systems designed for angiography applications, the radiation transparency and the maximum patient thickness that can be properly imaged would be lower for the traditional equipment.

No explicit image quality evaluation was included in this report, and no attempt was made to validate whether the tested programs were appropriate for the intended clinical procedures. Although it has been shown that the use of thick spectral filters is particularly beneficial for pediatric fluoroscopy,[67–69] where radiation sensitivity is a major concern,[70] there was no attempt made to determine if the equipment under study provided special programs for pediatric patients. Likewise, there was no attempt to determine if the use of increased spectral filtration could benefit the morbidly obese patient for which the potential for serious skin injury is a major concern.[71–73]

Finally, the work of TG-125 was limited to the fluoroscopic operation of the imaging equipment and did not include the acquisition modes (e.g., digital cine, digital angiography, DSA, etc.). Although the acquisition modes often utilize the same signal measurement and generator control logic as that for the fluoroscopic operation, there is generally greater user control over the selection of the EERD, spectral filtration, generator parameters, and image processing. Thus the acquisition mode of operation would be an important topic for additional study and evaluation.

XI. Acknowledgments and Disclaimer

Members of TG-125 sincerely appreciate valuable discussions provided by the engineers and scientists from (in alphabetical order) GE Healthcare, Hitachi Medical Systems, Philips Healthcare, Shimadzu Medical Systems, Siemens Healthcare, and Toshiba Medical Systems. Despite trade restrictions, the information provided by various individuals was very useful and assistance provided in looking into the hardware connection points and test points has ensured the accuracy of the imaging parameters being measured.

The authors appreciate and thank the IEC for permission to reproduce information from its international standard IEC 61267 ed. 2.0 (2005).

Acronyms and Abbreviations in TG-125 Report

AAPM	American Association of Physicists in Medicine
ABC	Automatic Brightness Control
ADRC	Automatic Dose Rate Control
ADRIQ	Automatic Dose Rate and Image Quality
AGC	Automatic Gain Control
AKR	Air Kerma Rate
Al	Aluminum
Au	Gold
CLT	Critical lead thickness
cm	Centimeter
Cu	Copper
DQE	Detective quantum efficiency
DSA	Digital subtraction angiography
EERD	Entrance exposure rate to the detector
EP	Electrophysiology
FDA	U.S. Food and Drug Administration
FOV	Field of view
fps	Frames per second
HU/sec	Heat Units per second
HVL	Half-value layer
IEC	International Electrotechnical Commission
kVp	Kilovolts peak
mA	Milliampere
μGy/s	Microgray per second
μR/s	Microroentgen per second
mGy/min	Milligray per minute
ms	Millisecond
NCRP	National Council on Radiation Protection and Measurements
NEMA-SCAI	National Electrical Manufacturers Association – Society for Cardiac Angiography
nGy/s	Nanogray per second
NIST	National Institute of Standards and Technology
NTSC	National Television System Committee
PAK	Patient Air Kerma
PAKR	Patient Air Kerma Rate
Pb	Lead
Pixel	Picture element
PMMA	Polymethylmethacrylate

pps	Pulses per second
PW	Pulse width
r	Grid ratio
rms	Root mean square
RQA	Radiation Qualities based on a phantom made up of an Aluminum added filter
RQR	Radiation Qualities in Radiation beams emerging from the x-ray tube assembly
R/min	Roentgen per minute
SEER	Skin Entrance Exposure Rate
SI	International System of Units
SID	Source–to–image receptor distance
SNR	Signal-to-noise ratio
$\mathbf{T_d}$	PMMA thickness to double the PAKR
TG	Task Group
TID	Tabletop–to–image receptor distance
XRII	X-ray image intensifier
Z	Atomic number

Appendix

TG-125 Data Collection Methodology

1. Position the C-arm in a vertical x-ray beam position, with the image receptor at the top position, x-ray tube beneath the table.
2. Position the dosimeter chamber on the tabletop, centered in the FOV.
3. Place a support block on each side of the ionization chamber for the purpose of supporting the PMMA sheets above the dosimeter.
4. Set the SID of the system to 120 cm (or maximum SID).
5. Position the tabletop vertically such that the dosimeter chamber is at the IEC reference point (15 cm below isocenter) as shown in Figure 8.
6. When collecting data, always initiate and stop a short "test" fluoroscopy exposure after a change in attenuator thickness and before collecting data. This step ensures that filter changeover will occur, if necessary, following a change in attenuator thickness.
7. If a filter change is detected following increased PMMA in the beam, remove the last 1-in. thick slab and increase the PMMA by four ¼-inch increments to determine more precisely the thickness and exposure factors associated with the filter changeover. Repeat step 6 with each increment of PMMA.
8. During fluoroscopy allow the parameters to stabilize, and then record the PMMA thickness, kVp, mA, PW, filter selected, and PAKR.
9. Plot the results as shown in Figure 9 and Figure 10 in order to characterize the generator power curve and the ABC/ADRIQ operational logic of the system.

References

1. R. Nicholson, F. Tuffee, M.C. Uthappa. "Skin sparing in interventional radiology: the effect of copper filtration." *Br J Radiol* 73:36–42 (2000).
2. R.E. Morrell, A.T. Rogers, J.C. Jobling, K.E. Shakespeare. "Barium enema: use of increased copper filtration to optimize dose and image quality." *Br J Radiol* 77:116–122 (2004).
3. R.B. Mooney and P.A. Flynn. "A comparison of patient skin doses before and after replacement of a neurointerventional fluoroscopy unit." *Clin Radiol* 61:436–441 (2006).
4. O. Dragusin, R. Breisch, C. Bokou, and J. Beissel. "Does a flat panel detector reduce the patient radiation dose in interventional cardiology?" *Radiat Prot Dosimetry* 139:266–270 (2010).
5. B.J. McParland and M.M. Boyd. "X-ray image intensifier performance and patient doses for combinations of supplemental beam filters and vascular contrast agents." *Phys Med Biol* 46:227–244 (2001).
6. L.K. Wagner. "Angiography Radiation Dose" In: *2006 Syllabus: Categorical Course in Diagnostic Radiology Physics: From Invisible to Visible—The Science and Practice of X-ray Imaging and Radiation Dose Optimization*. D.P. Frush, W. Huda (eds.) 92nd Scientific Assembly and Annual Meeting, Nov 26–Dec 1, 2006. Oak Brook, IL: Radiological Society of North America, 2006.
7. E. Guibelalde, E. Vañó, C.J. Kotre, K. Faulkner, J.M. Fernández, J.I. Ten, D.J. Rawlings. "The use of dynamic phantoms in interventional radiology." *Radiat Prot Dosimetry* 94:155–159 (2001).
8. E. Guibelalde, E. Vano, F. Vaquero, L. González. "Influence of x-ray pulse parameters on the image quality for moving objects in digital cardiac imaging." *Med Phys* 31:2819–2825 (2004).
9. J.M. Boone, D.E. Pfeiffer, K.J. Strauss, R.P. Rossi, P-J.P. Lin, J.S. Shepard, B.J. Conway. "A survey of fluoroscopic exposure rates: AAPM Task Group No. 11 Report." *Med Phys* 20(3):789–794 (1993).
10. P. Rauch. "The '30-30-30 Rule', a Practical Guide to Setting the Detector Input Exposure Rate for a Fluoroscopic Imager." [SU-GG-I-96] *Med Phys* 37:3123 (2010).
11. National Television System Committee. http://en.wikipedia.org/wiki/NTSC (Last accessed June 5, 2012).
12. Y. Srinivas and D.L. Wilson. "Image quality evaluation of flat panel and image intensifier digital magnification in x-ray fluoroscopy." *Med Phys* 29:1611–1621 (2002).
13. A. R. Cowen, A.G. Davies, MU Sivananthan. "The design and imaging characteristics of dynamic, solid-state, flat-panel x-ray image detectors for digital fluoroscopy and fluorography." *Clin Radiol* 63:1073–1085 (2008).
14. G.K. Yadava, A.T. Kuhls-Gilcrist, S. Rudin, V.K. Patel, K.R. Hoffmann, D.R. Bednarek. "A practical exposure-equivalent metric for instrumentation noise in x-ray imaging systems." *Phys Med Biol* 53:5107–5121 (2008).
15. Z. F. Lu, E. L. Nickoloff, C. B. Ruzal-Shapiro, J. C. So, A. K. Dutta. "New automated fluoroscopic systems for pediatric applications." *J Appl Clin Med Phys* 6:88–105 (2005).
16. E.L. Nickoloff, Z.F. Lu, A. Dutta, J. So, S. Balter, J. Moses. "Influence of flat-panel fluoroscopic equipment variables on cardiac radiation doses." *Cardiovasc Intervent Radiol* 30:169–176 (2007).
17. J. Fajadet, J. Marco, O. Bertel, E. Straumann. "Innovations in flat-detector cardiac angiography." *Medicamundi* 47/2 (2003).

18. S. Balter, F.A. Heupler, P-J.P. Lin, M.H. Wondrow. "A new tool for benchmarking cardiovascular fluoroscopes." *Cathet Cardiovasc Intervent* 52:67–72 (2001).
19. P. Sprawls. In: *Radiographic Image Formation and Characteristics, Physics: From Invisible to Visible—The Science and Practice of X-ray Imaging and Radiation Dose Optimization, Syllabus: Categorical Course in Diagnostic Radiology*. D.P. Frush, W. Huda (eds.). 92nd Scientific Assembly and Annual Meeting, Nov 26–Dec 1, 2006. Oak Brook, IL: Radiological Society of North America, 2006.
20. W.R. Geiser, W. Huda, and N.A. Gkanatsios. "Effect of patient support pads on image quality and dose in fluoroscopy." *Med Phys* 24:377–382 (1997).
21. J.W. Motz and M. Danos. "Image information content and patient exposure." *Med Phys* 5:8–22 (1978).
22. R.G. Zamenhof. "The optimization of signal detectability in digital fluoroscopy." *Med Phys* 9:688–694 (1982).
23. D.G. Onnasch, A. Schemm, H.H. Kramer. "Optimization of radiographic parameters for paediatric cardiac angiography." *Br J Radiol* 77:479–487 (2004).
24. L.K. Wagner, B.R. Archer, and A.M. Cohen. "Management of patient skin dose in fluoroscopically guided interventional procedures." *J Vasc Interv Radiol* 11:25–33 (2000).
25. 21CFR1020.32, *Code of Federal Regulations*, Title 21, Volume 8, Performance Standards for Ionizing Radiation Emitting Products: Fluoroscopic Equipment. Revised as of April 1, 2011.
26. B.R. Archer. "High-dose fluoroscopy: the administrator's responsibilities." *Radiol Manage* 24:26–32 (2002).
27. B.R. Archer and L.K. Wagner. "Protecting patients by training physicians in fluoroscopic radiation management." *J Appl Clin Med Phys* 1:32–37 (2000).
28. B.A. Schueler, T.J. Vrieze, H. Bjarnason, A.W. Stanson. "An investigation of operator exposure in interventional radiology." *Radiographics* 26:1533–1541 (2006).
29. E.D. Trout, J.P. Kelley, G. A. Cathey. "The use of filters to control radiation exposure to the patient in diagnostic roentgenology." *Am J Roentgenol Radium Ther Nucl Med* 67:946–963 (1952).
30. D. Gifford and D.E. Truscott. "The use of additional filtration in medical radiography." *Br J Radiol* 27:113–116 (1954).
31. A. den Boer, P.J. de Feyter, W.A. Hummel, D. Keane, J.R. Roelandt. "Reduction of radiation exposure while maintaining high-quality fluoroscopic images during interventional cardiology using novel x-ray tube technology with extra beam filtering." *Circulation* 89:2710–2714 (1994).
32. H.D. Nagel. "Comparison of performance characteristics of conventional and K-edge filters in general diagnostic radiology." *Phys Med Biol* 34:1269–1287 (1989).
33. H.D. Nagel. "Technical note: Dose management." *Medicamundi* 41:2 (1997).
34. A.L. Clark, A.G. Brennan, L.J. Robertson, J.D. McArthur. "Factors affecting patient radiation exposure during routine coronary angiography in a tertiary referral centre." *Br J Radiol* 73:184–189 (2000).
35. E. Vañó, L. González, E. Guibelalde, J. M. Fernández, J.I. Ten. "Radiation exposure to medical staff in interventional and cardiac radiology." *Br J Radiol* 71:954–960 (1998).
36. M. Sandborg, C.A. Carlsson, G.A. Carlsson. "Shaping X-ray spectra with filters in X-ray diagnostics." *Med Biol Eng Comput* 32(4):384–390 (1994).
37. M.J. Tapiovaara, M. Sandborg, and D.R. Dance. "A search for improved technique factors in paediatric fluoroscopy." *Phys Med Biol* 44:537–539 (1999).
38. R.M. Gagne, P.W. Quinn, R.J. Jennings. "Comparison of beam-hardening and K-edge filters for imaging barium and iodine during fluoroscopy." *Med Phys* 21(1):107–121 (1994).

39. R.F. Fleay, R.A. Fox, P.L. Sprague, J.P. Adams. "Dose reduction in paediatric radiology using rare earth filtration." *Pediatr Radiol* 14:332–334 (1984).
40. L. Duggan, H. Warren-Forward, T. Smith, T. Kron. "Investigation of dose reduction in neonatal radiography using specially designed phantoms and LiF:Mg,Cu,P TLDs." *Br J Radiol* 76:232–237 (2003).
41. S. Miyazaki, S. Abe, Y. Katoh, H. Kobayashi, H. Uehara. "[Evaluation of patient entrance dose rate of interventional X-ray equipment]." *Nihon Hoshasen Gijutsu Gakkai Zasshi* 59:839–847 (2003). [Japanese].
42. P.L. Rossi, M. Mariselli, I. Corazza, D. Bianchini, M. Biffi, C. Martignani, R. Zannoli, G. Boriani. "Decrease in patient radiation exposure by a tantalum filter during electrophysiological procedures." *Pacing Clin Electrophysiol* 32 (Suppl 1):S109–S112 (2009).
43. F. Thorsen, A. Mehus, J. Nordanger. "[The use of copper and niobium filters in diagnostic x-ray equipment. A comparison of dose reduction, tube loading and picture quality]." *Tidsskr Nor Laegenforen* 110:2878–2880 (1990). [Norwegian].
44. J.E. Villagran, B.B. Hobbs, K.W. Taylor. "Reduction of patient exposure by use of heavy elements as radiation filters in diagnostic radiology." *Radiology* 127:249–254 (1978).
45. E.L. Nickoloff and H.L. Berman. "Factors affecting x-ray spectra." *Radiographics* 13:1337–1348 (1993).
46. L. Verhoeven and E.G. Mast. "Coronary X-ray angiography: 40 years of experience." *Medicamundi* 43:46–54 (1999).
47. T. Schmidt and R. Behling. "MRC: a successful platform for future X-ray tube development." *Medicamundi* 44:50–55 (2000).
48. D. Holzman. Dose Reduction with C.A.R.E. Siemens Medical Solutions, October 2004.
49. R.M. Gagne and P.W. Quinn. "X-ray spectral considerations in fluoroscopy" In: *1995 Syllabus: Categorical Course in Physics—Physical and Technical Aspects of Angiography and Interventional Radiology.* S. Balter and T. B. Shope (eds.). Oak Brook, IL: Radiological Society of North America, pp. 49–58 (1995).
50. United States Patent 5,680,435. "X-ray diagnostic apparatus with a filter device." Johann Seissl, October 21, 1997.
51. P-J.P. Lin. "The operation logic of automatic dose control of fluoroscopy system in conjunction with spectral filters." *Med Phys* 34:3169–3172 (2007).
52. A. Fukuda, K. Koshida, I. Yamaguchi, A. Togashi, K. Matsubara. "[Method of estimating patient skin dose from dose displayed on medical X-ray equipment with flat panel detector]." *Nihon Hoshasen Gijutsu Gakkai Zasshi* 60(5):725–733 (2004). [Japanese].
53. A. Dowling, A. Gallagher, C. Walsh, J. Malone. "Equipment standards for interventional cardiology." *Radiat Prot Dosimetry* 117:79–86 (2005).
54. 21CFR1020.30, *Code of Federal Regulations,* Title 21, Volume 8, Diagnostic x-ray systems and their components. Revised as of April 1, 2011.
55. J.E. Gray, Video-based components. In: *1995 Syllabus: A Categorical Course in Physics—Physical and Technical Aspects of Angiography and Interventional Radiology*. S. Balter and T.B. Shope (eds.). Oak Brook, IL: Radiological Society of North America, pp. 117–120 (1995).
56. P-J.P. Lin. "Acceptance Testing of Automatic Exposure Control Systems and Automatic Brightness Stabilized Fluoroscopic Equipment" In: *Quality Assurance in Diagnostic Radiology*. R. G. Waggener and C.R. Wilson (eds.). AAPM Monograph No. 4. New York, NY: American Institute of Physics, pp. 10–27, 1980.
57. B. Belanger and J. Boudry. "Management of pediatric radiation dose using GE fluoroscopic equipment." *Pediatr Radiol* 36 (Suppl 2):204–211 (2006).

58. P.L. Rauch. "Acceptance Testing of Automatic Exposure Control Systems" In: *Acceptance Testing of Radiological Imaging Equipment*. P-J.P. Lin, R.L. Kriz, K.J. Strauss, P.L. Rauch, R. P. Rossi (eds.). AAPM Proceedings No. 1. New York, NY: American Institute of Physics, pp. 205–226, 1982.
59. P-J.P. Lin, "Acceptance Testing of Cine Imaging Systems for Cardiac Catheterization Laboratories" In: *Acceptance Testing of Radiological Imaging Equipment*. P-J.P. Lin, R.L. Kriz, K.J. Strauss, P.L. Rauch, R.P. Rossi (eds.). AAPM Proceedings No. 1. New York, NY: American Institute of Physics, pp. 227–240, 1982.
60. P-J.P. Lin. "Cine and Photospot Cameras" In: *Encyclopedia of Medical Devices and Instrumentation*, Vol. 2, New York, NY: Wiley Interscience, pp. 681– 693, 1988.
61. E. L. Nickoloff. "AAPM/RSNA physics tutorial for residents: physics of flat-panel fluoroscopy systems: survey of modern fluoroscopy imaging: flat-panel detectors versus image intensifiers and more." *Radiographics* 31:591–602 (2011).
62. Section 22.4, X-ray Beam Limiting Device (BLA-800C and BLA-900A), Operation Manual for Interventional Angiography System, Infinix©-i, Model INFL-8000V for Single-plane system (2B308-075EN*D), p. 327, Toshiba Medical Systems, Inc.
63. National Institute of Standards and Technology. X-Ray and Gamma-Ray Measuring Instruments (46010C-46110C) http://ts.nist.gov/MeasurementServices/Calibrations/x-gamma-ray.cfm#46010C (Last accessed June 5, 2012).
64. International Standard IEC 61267 ed. 2.0 (2005). Medical diagnostic X-ray equipment – Radiation conditions for use in the determination of characteristics. Geneva, Switzerland: International Electrotechnical Commission. http://www.iec.ch. (Last accessed June 5, 2012).
65. National Council on Radiation Protection and Measurements (NCRP) Report No. 168: Radiation Dose Management for Fluoroscopically-Guided Interventional Medical Procedures. Bethesda, MD: NCRP, 2010.
66. P-J.P. Lin. "Operation logic and functionality of automatic dose rate and image quality control of conventional fluoroscopy." *Med Phys* 36:1486–1493 (2009).
67. K.J. Strauss. "Cardiac Catheterization Equipment Requirements: Pediatric Catheterization Laboratory Considerations" In: *1998 Syllabus: Categorical Course in Diagnostic Radiology Physics—Cardiac Catheterization Imaging*. E.L. Nickoloff and K.J. Strauss (eds.). Oak Brook, IL: Radiological Society of North America, pp.105–120 (1998).
68. J.W. Fenner, G.D. Morrison, J. Kerry, N. West. "A practical demonstration of improved technique factors in paediatric fluoroscopy." *Br J Radiol* 75:596–602 (2002).
69. A.J. Gislason, A.G. Davies, A.R. Cowen. "Dose optimization in pediatric cardiac x-ray imaging." *Med Phys* 37:5258–5269 (2010).
70. N. Miksys, C.L. Gordon, K. Thomas, B.L. Connolly. "Estimating effective dose to pediatric patients undergoing interventional radiology procedures using anthropomorphic phantoms and MOSFET dosimeters." *AJR Am J Roentgenol* 194:1315–1322 (2010).
71. S.G. Bryk, M.L. Censullo, L.K. Wagner, L.L. Rossman,A.M. Cohen. "Endovascular and interventional procedures in obese patients: a review of procedural technique modifications and radiation management." *J Vasc Interv Radiol* 17:27–33 (2006).
72. J.C. Gurley. "Flat detectors and new aspects of radiation safety." *Cardiol Clin* 27:385–394 (2009).
73. S. Balter, J.W. Hopewell, D.L. Miller, L.K. Wagner, M.J. Zelefsky. "Fluoroscopically guided interventional procedures: a review of radiation effects on patients' skin and hair." *Radiology* 254: 326–341(2010).